EXPERIMENTAL INVESTIGATION AND MATHEMATICAL MODELLING OF A NATURAL CONVECTION SOLAR TUNNEL FRUIT DRYER

By

Cherotich Sam

A dissertation submitted in partial fulfilment of the requirements for the degree of Master of Engineering in Agricultural Engineering

The University of Zambia

July, 2016

DECLARATION

I, **CHEROTICH SAM** do hereby declare that the contents in this dissertation are my original work and have not been previously submitted to any University for the award of a degree or any other qualification.

Signature……Date……

CERTIFICATE OF APPROVAL

This dissertation submitted by **CHEROTICH SAM** is approved as fulfilling the requirements for the award of the degree of Master of Engineering in Agricultural Engineering at the University of Zambia.

. …….. …….

Supervisor Signature Chairperson (Board of Examiners) Signature

Examiner…… Sign…… Date…….

Examiner…… Sign…… Date…….

Examiner…… Sign…… Date…….

ABSTRACT

Post-harvest Losses (PHLs) in fruits are high, in some cases, reaches 50 %. To reduce these PHLs, several technologies have been developed; among them is solar drying technology (SDT). Several SDTs are available including solar tunnel dryers. Solar tunnel dryers are described as relatively simple, and easy to construct, and this formed the basis for choice of a solar tunnel dryer in this study. To achieve a good quality product and to identify any areas for improvement in a solar dryer, experimentation is necessary. The purpose of this study therefore was to investigate the performance of a natural convection solar tunnel fruit dryer and to determine an appropriate thin layer model to predict the drying. A solar tunnel dryer comprising three major units: a black painted solar collector unit, a drying unit and a black painted vertical bare flat-plate chimney was constructed. The overall dimensions of the collector unit and drying units were 2 m×0.75 m (L×W) while the chimney was square, measuring 0.75 m×0.75 m (H×W) with 0.1 m air exit channel. To investigate its performance, 5 mm thin layer drying experiments with mango, a major fruit in Zambia, were carried out at the University of Zambia, Department of Agricultural Engineering under natural conditions. To find an appropriate thin layer model, the moisture content results were transformed to Moisture Ratio (MR) and fitted into 12 common thin layer models in literature using MatlabR2011b curve fitting tool and the best model determined based on three statistical parameters: coefficient of determination (r^2), Sum of Square Error (SSE) and Root Mean Square Error (RMSE). The results showed that under solar insolation of between 470 and 1070 W m^{-2}, air temperature of up to 70 ^oC was attained at the collector unit. Ambient relative humidity varied between 11.95 and 29.67 % and was lowered by over 50 % at the collector unit. Under these conditions, mango with an initial moisture content of 80 % (w.b.) was dried to between 13 and 14 % (w.b.) in 11 hours. The performance of the dryer was analyzed by calculating the collector, drying, and pick-up efficiencies. They were found to be 24.7 %, 11.3 % and 35 % respectively which compared well with values for natural convection dryers in literature. The buoyancy pressure ranged from 0.1530 to 0.3016 N m^{-2} and was sufficient to drive the flow of air in all the experiments. Among the 12 thin layer models tested, Midilli-Kucuk model was the best with r^2, SSE and RMSE of 0.9959, 0.004634, and

0.01758 respectively. Based on the achieved drying time for the 5 mm mango slices, the collector and pick efficiencies, the dryer performed well. Further investigations using different fruits such as pineapple, banana and different slice thicknesses are recommended.

DEDICATION

This research work is dedicated to my family members for their prayers and unconditional support during the study period. May the almighty God bless and protect you all.

AKNOWLEDGEMENTS

I am highly grateful to my sponsors, Mobility to Enhance Training of Engineering Graduates in Africa (METEGA), first, for awarding me the scholarship to pursue a MEng-Agricultural Engineering at the University of Zambia and secondly, covering the tuition fees and the other necessary support such as medical insurance and a monthly stipend. Without these, this study would not have been possible.

Sincere appreciation goes to my supervisor Dr. Isaac N. Simate for his insightful input that helped me stay on track and to finish this project within the time frame allocated to the study. May the almighty God bless your endeavors.

I would also like to acknowledge the head of Department Agricultural Engineering, University of Zambia Dr. J.M Chileshe together with his entire members of staff, technical and support staff for their generous input. The progress presentations that were held at the Department enabled me to share the milestones from the study and in return received insightful comments that were relevant to the study.

To Prof. Reccab Ochieng Manyala, I am highly indebted to you for your exceptional input in this study given your vast knowledge in the field of solar energy. I look forward to receiving further mentorship from you as I plunge in to my career.

Last but not least, to my colleagues Rhoda (from Kenya), John (from Uganda), Luqman (from Ghana) and Lt. Col. Mukuwa (from Zambia); thank you guys for providing such a good atmosphere where knowledge, culture and issues pertaining to life were shared.

TABLE OF CONTENTS

LIST OF FIGURES

LIST OF TABLES

LIST OF ABRREVIATIONS

d.b.	Dry basis		**SUBSCRIPTS**
g	Acceleration due gravity, m s^{-2}	Exp	Experiment
GDP	Gross Domestic Product	Pred	Predicted
GI	Galvanized Iron	e	Equilbrium
H	Height of chimney, m	ch	Chimney exit
I_s	Solar insolation, W m^{-2}	c	Collector exit
LD	Loading Density	d	Dryer exit
M	Moisture content, %	am	Ambient
METEGA	Mobility to Enhance Training of Engineering Graduates in Africa	o	Initial
MR	Moisture Ratio		
MSE	Mean Square Error		
R^2	Regression coefficient		
N	Number of data points		
OSD	Open Sun Drying		
PHLs	Post-Harvest Losses		
r^2	Coefficient of determination		
RH	Relative Humidity, %		
RMSE	Root Mean Square Error		
SDT	Solar drying technology		
T	Air Temperature, ^oC		
t	Elapsed drying time		
v	Residual degrees of freedom		
w.b.	Wet basis		
ρ	Air density, kg m^{-3}		

CHAPTER ONE

1. INTRODUCTION

In this chapter, a background to the study, the statement of problem, the significance of the study, the study objectives, the scope of the study and finally closing remarks are presented.

1.1 Background

1.1.1 Agriculture and Economic development

Many economies especially in the developing countries derive a reasonable part of their economic growth from agriculture. In a report by the Food Agricultural Organisation (FAO), it was estimated that about 2.5 billion livelihoods worldwide depended on agriculture (FAO, 2013) and up to 30 % of the world Gross Domestic Product (GDP) came from agriculture (Hodges *et al.*, 2011). In 2010, Zambia had a total population of about 13 million people with about 70 % of the rural population being employed in agriculture (Kuteya, 2012). With this significant population involved in agriculture, the GDP contribution from agriculture in Zambia grew from 18 % in 2008 to 20 % in 2009 (FAO, 2013). Agriculture and its related support sectors therefore, are highly vital in economic development.

The main objective of the agricultural industry is to produce enough food for consumption. In an attempt to do so, it is faced with several challenges which stem from; (1) policy, (2) technology, (3) financial/economic, (4) climatic, (5) natural disasters and other factors. For the purposes of this study, technological challenges were of interest. In the context of this study, technological challenges refer to lack, inaccessibility, non-affordability, inappropriateness, or unawareness of existing technologies. These technologies take the form of software and hardware or tools that aid an efficient food production. It can be noticed that there exists relationships between the first three challenges stated above. There is therefore, interaction amongst these three challenges. One such interaction that may be pointed out is among policy, finance/budget allocation and technological developments. The interaction arises because budget allocations by governments have an enormous bearing on policies while both budget and policy have a bearing on technological development. Therefore,

addressing technological challenges should be in tandem with supporting policies to make significant and sustainable impacts.

In Zambia, the National Agricultural Policy vision (2004-2015) was to "promote development of an efficient, competitive and sustainable agricultural sector, which assures food security and increased income''(Mundia, 2004). In the context of technology, the policy aimed at developing and promoting appropriate technology for increased agricultural production and utilization. Benefits of increased agricultural production include increased chances of a food secure country and a potential increase in the household incomes.

1.1.2 Food security

The widely accepted description of food security is: "food security exists when all people, at all times, have physical and economic access to sufficient, safe and nutritious food that meets their dietary needs and food preferences for an active and healthy life" (Shaw, 2007).

Without food security, the productivity of a nation could be compromised because of the lack of or inadequate access to food by the productive workforce and consequently energy to do work. This suggests that attaining a food secure country among many other factors such as a healthy population and security is paramount to increasing the level of productivity in any country.

A number of factors are responsible for the lack of food security in many countries especially in sub-Saharan Africa. These factors include low productivity levels, use of poor technologies or in some cases lack of technologies, climate change, and the prevalent food loss and waste.

1.1.3 Food losses and food waste

Food losses refer to the reduction in the edible food mass along the food supply chain leading to the edible food for human consumption (Parfitt *et al.*, 2010) while food waste refers to "food appropriate for human consumption being discarded, whether or not after it is kept beyond its expiry date or left to spoil" (Kiaya, 2014).

From the above definitions, it is clear that both food losses and food waste lead to reduction in food available for human consumption. With significant food losses and

waste, there is an accompanying reduction in income or profit or food insecurity. Table 1.1 illustrates some of the stages and examples of food losses and food waste. Among the stages of food loss and food waste are; drying, handling, transportation and distribution as well as storage.

Table 1.1: Food loss and waste: Stages along the food production chain and examples

Stage	Examples of waste
1. Harvesting, handling at harvesting	*Edible crops left in field, ploughed into soil, eaten by pests; timing of harvest not optimal; crop damaged during harvesting*
2. Threshing	*Loss due to poor technique*
3. Drying, transport and distribution	*Quality and quantity loss of during drying, poor transport infrastructure; loss owning to spoiling/bruising*
4. Storage	*Pests and disease attacks, spillage, contamination; natural drying out of food*
5. Primary processing, cleaning, classification, hulling, pounding, grinding, packaging, soaking, winnowing, drying, sieving, milling	*Process losses; contamination in process causing loss of quality.*
6. Secondary processing, mixing, cooking, frying, molding, cutting, extrusion	*Process losses; contamination in process causing loss of quality*
7. Product evaluation and quality control	*Product disregarded /out-grades in supply chain*
8. Packaging	*Inappropriate packaging damages produces; grain spillage from sacks; attack by pests*
9. Marketing, selling, distribution	*Damage during transport; spoilage; poor handling; losses caused by poor storage*
10. Post-consumer	*Poor storage/stock management; discarded before serving; poor food preparation; expiration*
11. End of life disposal of food waste/loss at different stages in supply chain.	*Food waste discarded may be separately treated, fed to animals, mixed with other wastes/landfilled*

Source: (Parfitt *et al.*, 2010)

Global food waste figures are reported at about one-third of the edible parts of food produced for human consumption (FAO, 2013). This is about 1.3 billion tonnes of food losses and waste annually. With a per capita food production of 460 kg/year, sub-Saharan Africa registered a per capita food loss of 120-170 kg/year (FAO, 2013). The study further indicated that in most low-income countries, where most African countries fall, food losses were more at the early and middle stages of the food supply chain than at the consumption stage. The food losses and waste came from both crop and animal production chains. Significant reduction in these food losses is therefore

paramount to increasing the amount of food available for consumption and a subsequent boost in food security.

Despite the significant amounts of food losses in the food production chain, much effort and resources have gone into food production in the past decades (Kader, 2004; Kitinoja *et al.*, 2010). These studies pointed out that in the past 30 years, about 95 % of the research investment has been directed towards increasing food production against only 5 % for reducing food losses. However, skewing most of the effort to only boosting food production in an attempt to increase food production and hence, food available for consumption may not entirely solve the challenge. This is because the world population continues to grow amidst limited land, water and other resources accompanied by unpredictability in the weather patterns mostly attributed to climate change. A possible way to achieve the goals of food security could be in reducing the food losses and waste especially after the post-harvest stage.

1.1.4 Post-harvest losses

Post-Harvest Losses (PHLs) refers to the measurable qualitative and quantitative food loss along the supply chain beginning from harvest to the final consumer (Hodges *et al.*, 2011). PHLs as mentioned, occurs in two forms namely, quantitatively and qualitatively. In quantitative PHLs, there is a decreased volume and weight in the food while qualitative PHLs are characterised by diminished nutrient value, undesirable changes in taste, odour, and textural change occurs. Due to the perishable nature of most fruits and vegetables, their PHLs are high.

In Zambia, especially in Soweto market in Lusaka, there are a number of situations that contribute to PHLs in fruits and vegetables (Hichaambwa, 2010). There are situations when supply exceeds demand for product in season resulting in subsequent losses in the quality of product. There are also cases attributed to inadequate processing facilities which translate to great wastage of fruits among them, guavas and mangoes. Generally, PHLs in the developing or developed countries are estimated to vary widely from 10 % to 80 % (Simon, 2011).

For fruits and vegetables the PHLs are estimated to be as high as 50 % of their production (Kiaya, 2014). Therefore there is need for an affordable and efficient means to reduce the PHLs with potential benefits being; income boost among the stake

holders in the fruit and vegetable industry and boosting of food security, a vital component in national development.

1.1.5 Technologies to reduce PHLs

Technologies such as (1) drying, (2) refrigeration, (3) modified atmosphere, and (4) cold storage have been applied to reduce PHLs in many products including fruits and vegetables. However, refrigeration, modified atmosphere and cold storage primarily demand reliable sources of energy for satisfactory results. Other major shortfalls associated with these techniques are; their high overall cost arising from the initial cost of the equipment, high running and maintenance costs, and the need for a relatively skilled workforce for efficient installation and operation. Due to these shortfalls, most of these technologies become highly restrained options to reducing PHLs especially in developing countries such as Zambia where incomes are quite low. However, the drying technology may be considered relatively cheaper because of its less energy demand compared to the other three technologies. Drying also is flexible in terms of energy sources with free sources such as solar energy having a huge potential. For this reason, this study focused on solar drying technology as it is sustainable.

1.1.6 Solar drying technology over open sun drying

Both solar drying and open sun drying (OSD) rely on the energy from the sun. The fundamental difference however, is in the use of equipment in solar dryers (Brenndorfer *et al.*, 1987). In a simple case, the equipment could take the form of a box with an absorbing plate covered in a clear plastic sheet. The result of such an arrangement is enhanced solar radiation. The enhanced solar radiation in solar dryers results in higher air temperatures and lower relative humidity favourable for drying. This is not the case in OSD.

Solar drying has been applied to a range of products including; cereals, nuts, oil crops, fruits and vegetables among others. Solar drying of fruits is one way of keeping fruits in a good quality for consumption and for any required subsequent processing. However, fruit drying is not a common practice especially in developing countries like Zambia. This may be attributed to inadequate knowledge and skills of fruit drying, lack of appropriate drying technologies, unaffordability of existing technologies, etc.

Generally, fruit drying is not a complex process largely because of the viability in use of inexpensive and non-sophisticated drying technologies such as solar drying. Since drying has associated costs, it is necessary to make it as cheap and efficient as possible to achieve a high quality product, and most importantly minimise the associated costs of energy, equipment, and labour among others. If all costs are brought to a minimum, the potential for a high profit margin is increased.

Solar dryers can be fabricated using locally available materials and with relatively simple skills. A study by Purohit *et al.* (2006), recommends that for drying of fruits and vegetables, it is highly vital to design a low cost dryer and using locally available materials and skills. This serves well the needs of most developing countries like Zambia with low income status and skills.

1.1.7 Mathematical modelling of solar dryers

Mathematical modelling in solar drying is diverse and broad. It includes; modelling the moisture diffusivity process, thin layer modelling of drying characteristics of products, and modelling for optimization of the dryer geometry (Hossain *et al.*, 2005; Simate, 2003; Sacilik *et al.*, 2006). The focus of this study was on thin layer mathematical modelling of the product dried in a natural convection dryer. Thin layer drying modelling contributes to understanding of the drying characteristics of the product being dried and therefore provides a viable way to control drying (Lahsasni *et al.*, 2004). By controlling the drying process, a quality product that can fetch a good price in the markets can be obtained.

1.2 Statement of the problem

Fruits are highly perishable and therefore their PHLs are high. In Zambia, the PHLs of fruits is estimated to be at 50 % annually (Phiri, 2010). Among these fruits are mangoes, bananas, pineapples etc. Some of the reasons to explain the high losses are; poor harvesting technologies, lack or under-developed handling and *processing technologies*, and failure of the market to consume most of the supply during the harvest season. *Solar drying technology* is an effective method in reducing PHLs in fruits. However, solar dryers require careful design and experimentation to determine the drying time, solar insolation, attainable air conditions such as temperatures, relative humidity and air speed for optimum drying in order to obtain a high quality product.

Through conducting an experimental investigation of a natural convection solar tunnel dryer, a simple, affordable and sustainable technology suitable for both small scale and commercial fruit farmers to dry mango as a preservation technique will be available. Furthermore, the thin layer mathematical model that will be established will enable prediction of the drying process and hence, enhances control of the drying process e.g determining when to stop the drying process.

1.3 Significance of the study

Through providing a simple and affordable solar drying technology in the form of a solar tunnel dryer, this study envisages to promote the growth of the local fruit solar drying industry. The growth of a local fruit drying industry will ultimately enhance the efforts of reducing PHLs in fruits. Furthermore, significant reductions in PHLs will boost incomes of fruit farmers, and food security in Zambia.

1.4 Objectives of the study

1.4.1 Main Objective

To investigate the performance of a natural convection solar tunnel dryer using mango as the product under natural weather conditions of Lusaka, Zambia.

1.4.2 Specific Objectives

The specific objectives of the study were:

i. To construct a natural convection solar tunnel dryer for experimentation,
ii. To determine an appropriate mathematical thin layer model to predict the drying characteristic of mango and validate it against experimental results and
iii. To evaluate the collector efficiency, drying efficiency, pick-up efficiencies and attainable buoyancy pressure by the chimney.

1.5 Scope of the study

This study reviewed literature from similar studies and existing types of solar dryers. From the review and considering the local availability of materials, procurement of the selected materials was done and the dryer was constructed. Finally, the experiments

were done from the constructed dryer using mango as a product and a mathematical thin layer model determined, and validated against experimental results.

The mathematical modelling aspect was on the thin layer drying of the product and not modelling of dryer design. The mathematical thin model was established from models existing in literature and validated against experimental results.

1.6 Closing remarks

An introduction to the topic has been presented and it highlights the relationship between PHLs and food security. The chapter further discussed briefly the current technologies available to reduce PHLs in fruits with solar drying among these technologies. A brief introduction to mathematical modelling has been highlighted in section 1.1.7 and finally, the problem which the study sought to address, the objectives of the study, and the scope have all been covered in this chapter.

CHAPTER TWO

2. LITERATURE REVIEW

In this chapter, an overview of solar energy reception on the earth, harnessing and its relevance is highlighted. A brief account of the drying rate, concept of equilibrium moisture content have been highlighted. The chapter further presents the various types of solar dryers in literature, their configurations and some materials used to make them. The chapter narrowed to solar tunnel dryers, their construction and experimentation. Finally, thin layer drying and mathematical modelling and the summary of the reviews close the chapter.

2.1 Overview

2.1.1 Solar energy reception and its relevance

Solar energy is the energy released from the sun in form of solar radiation. The sun produces this energy every day, and in only one hour, the solar energy is capable of meeting all the world energy demands (Mackay, 2015). Due to its incredible amounts, solar energy is known to drive all natural cycles and processes on the earth. Such processes include; rain formation, wind movement, and photosynthesis among others. These processes especially rain formation and photosynthesis are highly vital for life on the earth.

In order to make use of solar energy for engineering purposes, knowledge of its availability and intensity is required. Solar intensity and frequency of occurrence are specific to different geographic locations and hence, knowledge of it is vital for proper design of solar energy harnessing devices such as solar collectors for a specific purpose.

2.1.2 The Solar constant

The solar constant is the energy from the sun per unit time received on a unit area of surface perpendicular to the direction of propagation of the radiation at a mean Earth–Sun distance outside the atmosphere (Duffie and Beckman, 1980). The intensity of solar radiation outside the atmosphere averages a value of 1360 W m^{-2} and this value is known as the solar constant (Gayanilo, 1980).

Figure 2.1 illustrates the concept of the solar constant determination. Due to the presence of dust, water vapour molecules and ozone in the earth's atmosphere, total solar radiation from the Sun is scattered yielding a diffuse component of solar radiation (Brenndorfer *et al.*, 1987).

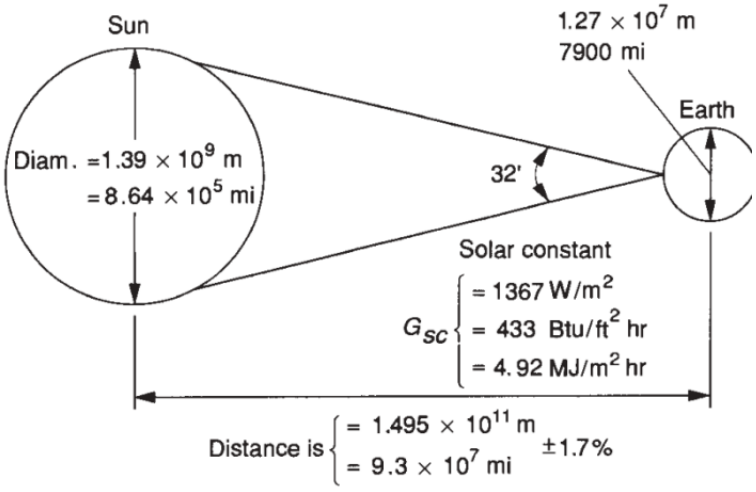

Figure 2.1: Sun–earth relationships (Duffie and Beckman, 1980)

Therefore the total solar energy reception on the earth's surface is a sum of direct and diffuse components. Some of the definitions relevant to understanding the concepts of solar energy reception on the earth are presented in Appendix XI.

Zambia being in the tropics receives plenty of solar energy throughout the year. Figure 2.2 shows the variation of solar radiation in different parts of Zambia.

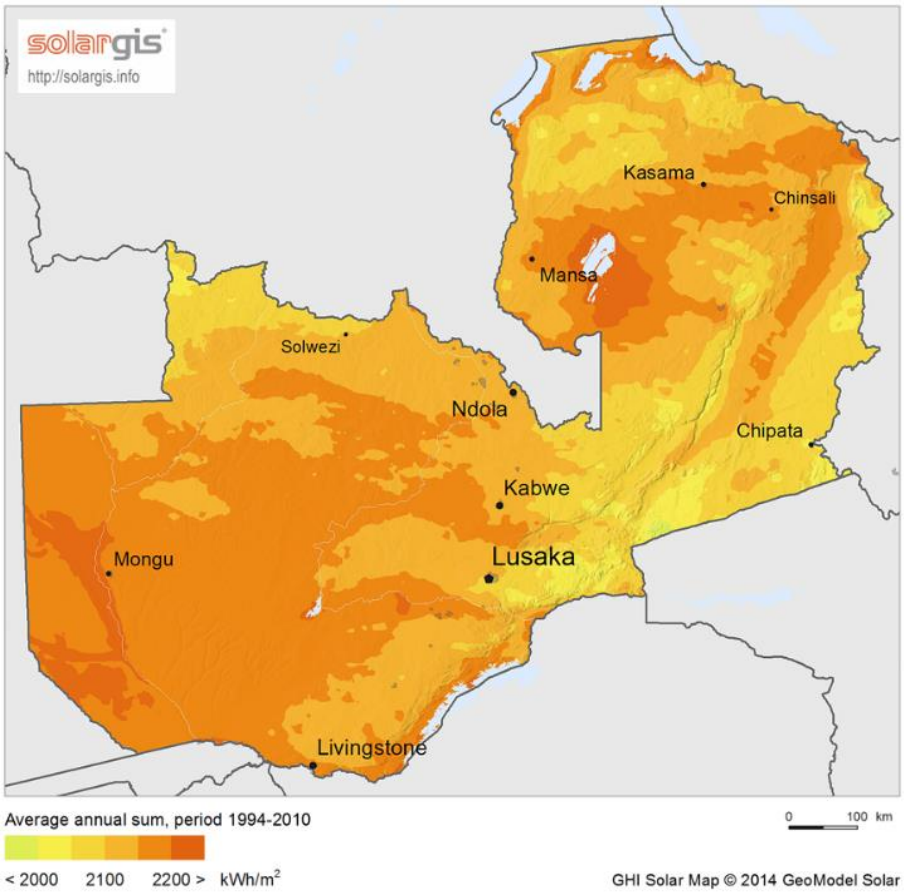

Figure 2.2: Global horizontal irradiation in Zambia (Source: SolarGIS maps, 2014)

From Figure 2.2, it can be observed that the annual global solar insolation in most parts of Zambia is over 2100 kWh/m^2 compared to only an average of 1100 kWh/m^2 in Northern Europe (Weiss and Buchinger, 2012). Zambia therefore, receives about twice as much solar insolation, heightening the potential of solar energy for solar drying in Zambia. A comparison of Lusaka, the study area and Mongu shows that Lusaka receives less solar insolation than Mongu and this suggests that if all conditions that affect drying are held constant, the same product would be dried much faster in Mongu than in Lusaka.

2.1.3 Drying, equilibrium moisture content and drying rate

In the context of foodstuff, drying is the simultaneous process of heat transfer to the product and mass transfer of the moisture from the interior of the product to its surface, and from the surface to the surrounding air (Mujumdar and Devahastin, 2000). The process continues until the vapour pressure of the moisture within the product equals that held in the atmosphere within the products. The moisture content when the

product moisture is equal to that of the surrounding environment is referred to as the product *equilibrium moisture content*.

The rate of moisture removal is termed as the drying rate. The drying rate is dependent on factors such as the temperature of the product, moisture content of the product, temperature, relative humidity and velocity of the drying air (Belessiotis and Delyannis, 2011). Figure 2.3 gives a general picture between the drying rate and the drying time.

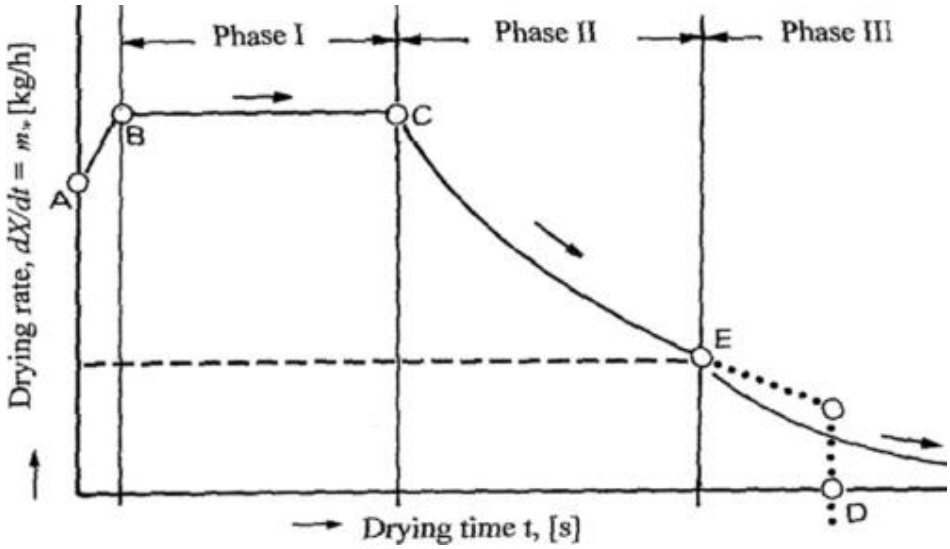

Figure 2.3: Global horizontal irradiation in Zambia (Source: SolarGIS maps, 2014)

As depicted in Figure 2.3, the drying rate is marked by two distinct phases; the constant rate period (Phase I) and the falling rate periods (Phases II and III). In the constant rate phase, the surface of the product is saturated with vapour and evaporation takes place continuously whereas in the falling rate period, the surface of the product is not saturated and the moisture diffusion is controlled by internal liquid movement as the surface dries. The second falling rate (phase III) is typical of hygroscopic products. In this phase, the moisture content decreases until equilibrium is attained at which point the drying ceases.

2.1.4 Open sun drying (OSD)

Traditionally, drying is done through OSD, a process mainly used to refer to drying of a product in the sun on a suitable surface. While OSD requires relatively little investment in terms of capital and expertise or skills to yield a product with an acceptable quality in reliable climates, it is marked by several limitations.

These limitations include; intermittent loss of moisture, low drying rates that lead to increased risk of spoilage, requirement of large open drying space, exposure of the product to insects and pests leading to damage of the product, contamination from foreign material such as dust and leaves, exposure of the product to rain, mycotoxin development and others. These limitations highly reduce the chances of achieving a good quality product.

Without a quality product, it is difficult for the dried product to fetch or compete for good price at the market. As an improvement on OSD, solar dryers have been developed. Solar drying is an effective means of food preservation because the product is completely protected during the process against rain, dust, insects and animals (Belessiotis and Delyannis, 2011). Therefore, solar drying as a drying technique results in a high quality product as compared to OSD. To harness solar energy for solar drying purposes, a means of collection is vital, and solar collectors have been used to achieve this.

2.2 Solar heat collectors

A solar heat collector is a unit used for harnessing solar energy and converting it to heat energy to heat a medium such as air (Ekechukwu and Norton, 1999b). There are two major categories of solar heat collectors; the concentrating type and the non-concentrating (flat-plate) type (Soponronnarit *et al.*, 1990).

The concentrating type solar collectors are equipped with a focusing reflector of a specific shape to increase the intensity of solar radiation on the absorbing surface and therefore, do generally attain higher temperatures than flat-plate type. Concentrating collectors are defined in terms of their concentrating ratio while flat-plate collectors are characterized by their efficiency. The concentration ratio is defined as the ratio of the aperture area to the absorber area (Mackay, 2015). The concept of the concentration ratio is illustrated in Figure 2.4.

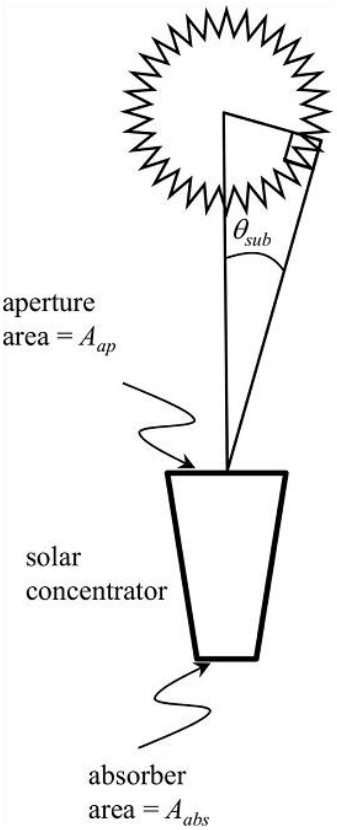

Figure 2.4: Global horizontal irradiation in Zambia (Source: SolarGIS maps, 2014)

The concentrating collectors are of two types and they are; the tracking concentrators and the non-tracking concentrators. The non-tracking concentrating collectors have a typical concentration ratio of 25 while the tracking concentrating collectors achieve concentration ratios between 50 and 80 (Mackay, 2015). Concentrating collectors are mainly designed for temperature rise of the working fluid greater than 100 ^{o}C above ambient whereas flat-plate collectors are suitable for moderate temperature rise of up to 100 ^{o}C above ambient temperature (Brenndorfer *et al.*, 1987; Weiss and Rommel, 2008).

Despite the ability of the concentrating collectors to achieve much higher temperatures than flat-plate collectors, the concentrating type are generally more complex than the flat-plate type (Soponronnarit *et al.*, 1990). For crop drying applications, the flat-plate type can attain adequate crop drying temperatures (Brenndorfer *et al.*, 1987). For these reasons, the flat-plate collectors have been reviewed further for the purposes of this study.

2.2.1 Flat-plate collectors, performance and their selection

Flat-plate collectors are distinctly defined by an absorbing surface purposed to receive the solar radiation and an air duct to channel the heated air to the desired destination (Soponronnarit *et al.*, 1990). The air duct is formed by a clear cover (may be glass or clear plastic sheet) over the absorber and one side of the absorber plate.

There are two major types of flat-plate collectors. These are; the *bare-plate* (shown in Figure 2.5) and *covered-plate* (shown in Figure 2.6) solar energy collectors (Brenndorfer *et al.*, 1987; Ekechukwu and Norton, 1999b). Figure 2.5 is an illustration of the bare-plate type of air heater while Figures 2.6 (a) and 2.6 (b) are types of covered-plate solar collectors.

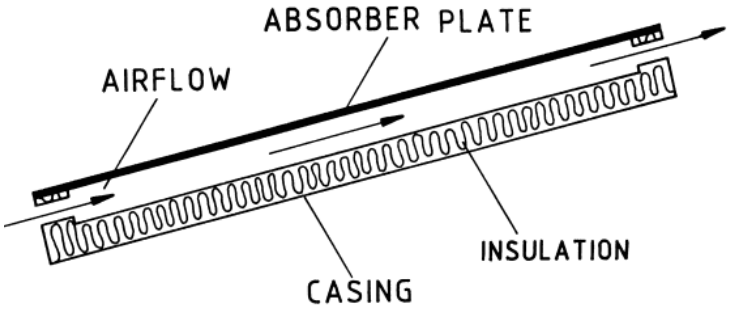

Figure 2.5: Bare-plate air heating solar collector (Source: Ekechukwu and Norton, 1999b)

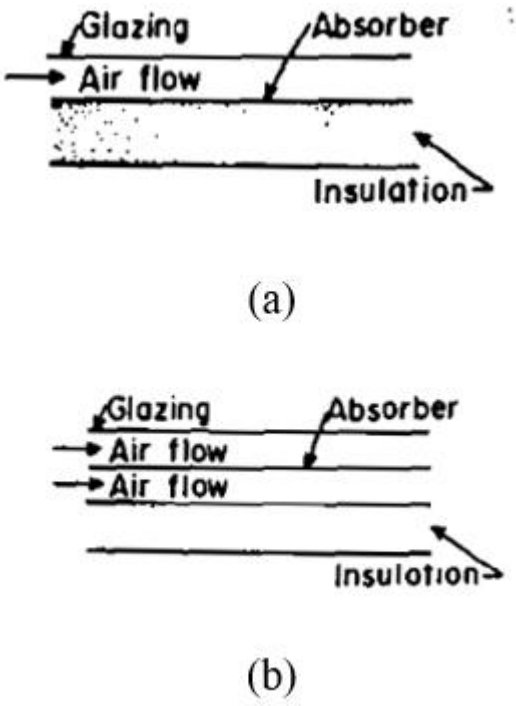

Figure 2.6: Bare-plate air heating solar collector (Source: Ekechukwu and Norton, 1999b)

The choice of a particular type of flat-plate collector for a specific purpose depends on the associated advantages and disadvantages. In Table 2.1, some of the advantages and disadvantages of the bare-plate collectors and covered-plate collectors are presented.

Table 2.1: Flat-plate collectors, advantages and disadvantages of each

Type of collector	**Advantages**	**Disadvantages**	**Reference**
Bare-plate air heating solar collector	□ Simple and cheap in construction □ Minimum optical losses	□ Huge thermal losses on the exposed surface □ Low temperature rise	(Soponronnarit et al., 1990; Ekechukwu and Norton, 1999b)
Covered-plate solar collector	□ High thermal efficiency due to covering	□More difficult in construction and more expensive due to cover □ High temperature rise	(Soponronnarit et al., 1990)

The performance of an absorber plate of a solar collector is influenced by four parameters that include; the level of insolation, the angle of incidence of solar radiation at the absorber surface, the absorptivity of the absorber surface, and the transmissivity of the cover material (Brenndorfer *et al.*, 1987). The influence of each parameter on the performance of a solar collector has been analysed (Ekechukwu and Norton, 1999b). In brief, they found out that the higher the insolation, the higher the energy absorbed by the collector. For transmittance, clear covers with transmissivity close to 1 transmitted much of the insolation to the absorber than covers with transmissivity close to 0, and hence high transmissivity materials enhance the performance of solar collectors. Black painted absorber plates have high absorptivity and therefore to enhance absorption of solar radiation, the absorber plates of solar collectors are usually painted black.

The overall performance of a flat-plate collector is obtained through evaluation of the *collector efficiency* which is a measure of the efficacy of transfer of the solar insolation incident upon the collector to the air flowing through the collector (Tiris *et al.*, 1995). The flat-plate collector efficiency ranges between 40% and 60 % depending on the air mass flow rate, the specific heat capacity of the air, the solar insolation and the temperature rise (Ahmad *et al.*, 1996).

In solar dryers, flat-plate collectors are integral units for the purpose of heating the air required for drying the product. The air temperature rise above ambient desirable for product drying helps designers of solar dryers to choose between the different flat-plate collectors described in Table 2.1. If an air temperature rise of only up to 10 ^{o}C above ambient is required, bare flat-plate collectors are the appropriate choice for use while for much higher temperature rise above ambient of up to 35 ^{o}C, covered flat-plate collectors are the appropriate choice (Brenndorfer *et al.*, 1987). The following section discusses the different types of solar dryers available.

2.3 Classification of solar dryers

Solar dryers have been categorised according to the air heating mode, mode of air flow, attainable air temperature rise, and their configurations. According to the mode of air flow, solar dryers have been classified as *active solar* drying systems and *passive solar* drying systems (Ekechukwu and Norton, 1999a; El-Sebaii *et al.*, 2002; Sharma *et al.*,

2009; Belessiotis and Delyannis, 2011). Under these two major classifications of solar dryers, Leon *et al.* (2002) proposed sub categorizations as described in Figure 2.7.

In Figure 2.7, both the passive and active solar drying systems are further subdivided into; direct mode, mixed mode, indirect mode, box-type, cabinet type, and tunnel dryers. The direct mode, the indirect mode and mixed mode have been described comprehensively in some studies (Simate, 2003; Forson *et al.*, 2007).

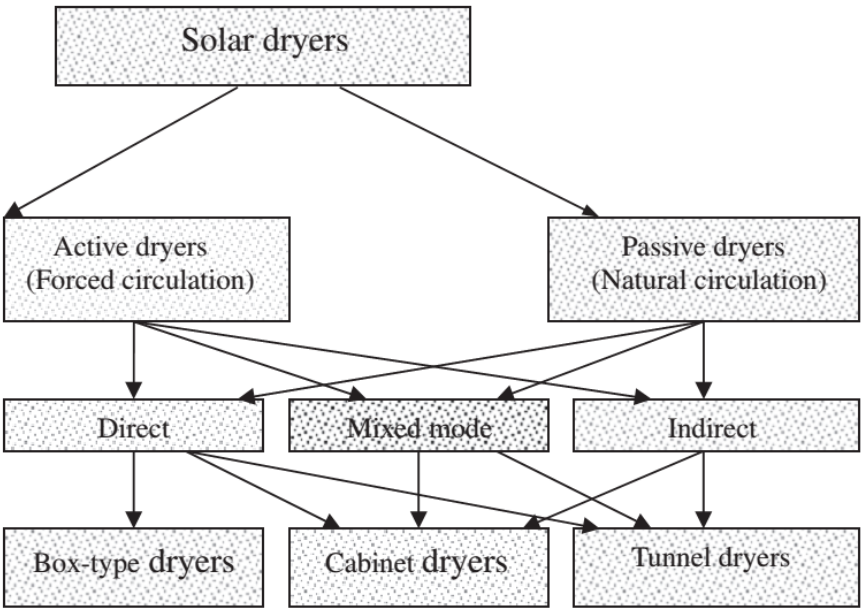

Figure 2.7: Classification of solar dryers based on design and heating mode

In the direct mode dryers, the product is contained in the same unit where the air is heated such that the solar radiation penetrating a transparent cover heats both the product and the air. For the indirect mode type, there is a distinct air heating unit and a drying unit. Air is preheated before drying the product in the drying unit. Finally, the mixed mode dryers have the air heated in two stages, firstly, at the air heating unit and secondly, at the product drying unit. Therefore in the mixed mode dryers, the product being dried benefits from direct solar energy falling on the drying unit, covered by a transparent cover and the pre-heated air from the air heating unit called a solar collector.

Despite the several sub-classifications of solar dryers as described Figure 2.7, several designs and configurations continue to be developed over the years, some through empirical constructions and hence, these types of dryers are difficult to classify exhaustively (Belessiotis and Delyannis, 2011). The following section discusses the two broad categories of active and passive solar dryers.

2.3.1 Active or Forced Convection Solar dryers

Active solar dryers are incorporated with a fan or a blower to force the air through the product contained in the dryer, hence, the term *forced convection* (Leon *et al.*, 2002; Fudholi *et al.*, 2010).

The major advantage of forced convection systems is their high efficiency in air movement. This makes active solar dryers suitable for drying large amounts of material and high moisture content products such as grains, papaya, cabbage, kiwi and others (Leon *et al.*, 2002; Sharma *et al.*, 2009).

The requirements for a fan and a source of power to drive the fan make active solar dryers more complex and relatively more expensive than passive solar dryers (Fudholi *et al.*, 2010). In most rural areas in developing countries such as Zambia, access to grid electricity is still lacking while areas with access are prone to moderate to severe load shading. Limitation in the viability of a grid powered fan in an active solar drying system is hence apparent.

Harnessing solar energy through a solar PV module employing a solar powered fan could be a much viable option for active solar drying systems in areas without access to grid electricity. However, using a solar PV module to power a fan in an active solar dryer has some downsides which include among others; high initial cost, and high chances of theft of the PV module if the system is to be operated in a field setup remote from close monitoring. The focus of this study was on *passive solar drying systems*, which require no fan but rely on buoyant air movement to drive the drying air through the product.

2.3.2 Passive or Natural Convection Solar dryers

Natural convection solar drying systems rely on solar energy for their operation (Simate, 2003; Fudholi *et al.*, 2010). The air heated by the solar energy becomes less dense than the ambient air resulting in a difference in air densities which in turn creates a buoyancy force. The buoyancy force or wind pressure or both causes air to be driven in and out of the dryer (Sharma *et al.*, 2009). The principle of natural convection is illustrated in Figure 2.8.

The hot object, which for the case of solar dryers is an absorber plate heats the cold air in its surrounding and hence, its temperature drops as a result of heat transfer to the air

while the temperature of the cold air rises. With continued heat transfer to the cold air, the hot object becomes surrounded by a layer of warm air. The warm layer of air consequently heats the adjacent layers of air creating a difference in density between the warm and cold air. The net result is that warm air rises and thus *natural convection* occurs.

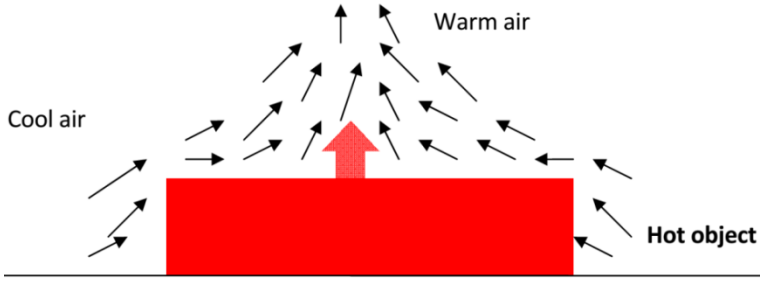

Figure 2.8: Natural convection heat transfer from a hot body (Sparrow and Bahrami, 1980)

The performance of both passive and active solar dryers is dependent on several parameters. These parameters scope from the characteristics of the product being dried, the weather conditions, the amount of solar radiation received and even the design of the solar dryer itself. The following section highlights some parameters used for evaluating the performance of either active or passive solar dryers.

2.4 Drying efficiency and pick-up efficiency

2.4.1 Drying Efficiency

The drying efficiency is a parameter that indicates the overall performance of the solar dryer and it is defined as the ratio of energy required to evaporate the moisture to the energy supplied for drying (Brenndorfer *et al.*, 1987). Mathematically, the drying efficiency is described by Equation (2.1).

$$\eta_{drying} = \frac{WL}{I_{ST} A_c} \qquad (2.1)$$

Where; η_{drying} is the drying efficiency, W is the total moisture removed in kg, L is the latent heat of vaporization of water at the dryer air temperature in J/kg and I_{ST} is the total solar insolation registered for the drying time.

The major parameters that influence the drying efficiency include the temperature of the air in the drying unit, the air flow rate, the air speed and the collector design (Leon *et al.*, 2002). Considering these parameters under the same solar insolation for a passive drying system and an active drying system, it can be pointed out that passive drying systems tend to have a lower drying efficiency than active solar drying systems. This is because there is no control on the air flow rates in passive drying systems, hence they normally tend to suffer low flow rates.

In this study, the drying efficiency is one of the indicators used to evaluate the performance of the solar tunnel dryer. Depending on the obtained drying efficiency, a decision can be made on what needs to be adjusted to enhance the efficiency.

2.4.2 Pick-up Efficiency

The pick-up efficiency is another important parameter in the evaluation of solar dryers that considers the evaporation of the moisture from the product. Precisely, the pick-up efficiency is a measure of the capacity of the heated air to absorb the moisture from the product (Brenndorfer *et al.*, 1987). It is defined mathematically using Equation (2.2).

$$\eta_{pick-up} = \frac{h_d - h_c}{h_{as} - h_c} \qquad (2.2)$$

Where; $\eta_{pick-up}$ is the pick-up efficiency, h_d is the absolute humidity of the air leaving the drying unit in kg/kg, h_c is the absolute humidity of the air leaving the collector unit and entering the drying unit in kg/kg and h_{as} is the adiabatic saturation humidity of the air entering the drying unit, kg/kg

Through experiments, it has been found out that the pick-up efficiency varies widely depending on the product being dried, the air flow rate and the relative ease with which the moisture can be evaporated from the product (Tiris *et al.*, 1995). In their study, an average pick-up efficiency of 42 % was obtained while drying products such as chilli, sultana grapes, beans and sweet peppers under air flow rates varying between 0.042 kg/m^{2}s and 0.07 kg/m^{2}s. From the definition of pick-up efficiency and the results of the study reviewed, it can be pointed out that the surface area of the product exposed to the drying air has an effect on the pick-up efficiency.

For passive solar dryers, the chimney unit can be evaluated by the amount of air temperature rise attained and the developed buoyancy pressure. In the next section, solar chimneys that have been applied in solar dryers are reviewed.

2.5 Solar chimney and estimation of buoyancy pressure

A solar chimney is a component in a passive solar drying system which serves the purpose of heating the air as a solar collector and help in creating air flow. The configurations of solar chimneyes vary based on the desired conditions such as temperature rise, cost and prevailing climatic conditions among others. Figure 2.9 shows a schematic of an existing design of a solar chimney for solar crop drying.

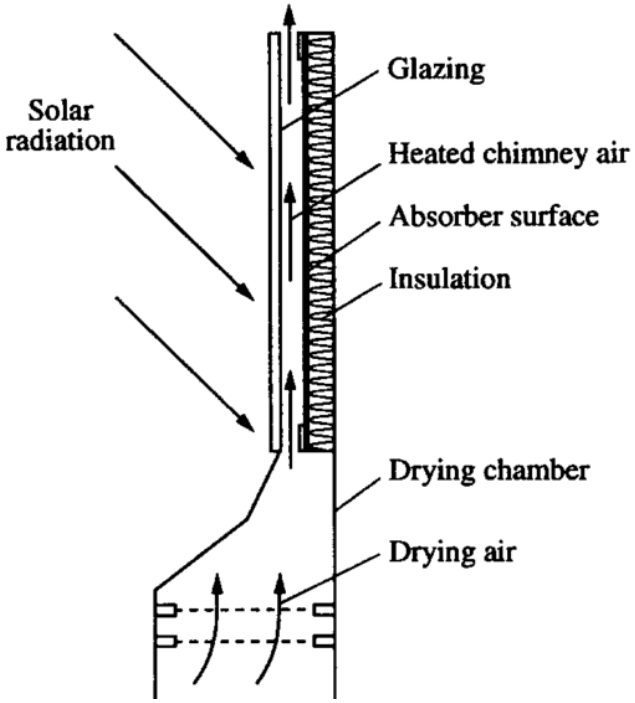

Figure 2.9: Air heating flat-plate solar energy chimney

The design of the chimney in Figure 2.9 is characterised by an insulated vertical plate covered in glazing to form a flat-plate air heating collector. The solar radiation falling through the glazing to the chimney absorber plate is converted in to heat energy. The heat energy of the absorber plate is then lost to the air by convective transfer and this causes the air within the chimney channel to become less dense compared to the ambient air. This difference in density is what results into the buoyancy pressure air flow defined mathematically as in Equation (2.3) (Brenndorfer *et al.*, 1987).

$$\Delta P_b = gH(\rho_{am} - \bar{\rho}_{ch}) \quad (2.3)$$

Where; ρ_{am} and $\bar{\rho}_{ch}$ are the densities of air in the ambient and air flowing in the chimney respectively in kg/m^3, g is the acceleration due to gravity in m/s^2 and H is the height of the chimney (m). Equation (2.3) was derived on the assumptions that air density inside the chimney was uniform throughout the chimney length and that there is no leakage of air from the system except for the warm less dense air exiting at the outlet.

The work of Brenndorfer *et al.* (1987) showed that with ambient air temperature of 25 ^{o}C and 60 % relative humidity, a chimney height of only 2.45 m was sufficient to achieve a temperature rise of 15 °C above ambient. This suggests that the height of the chimney has a profound role in defining the temperature rise in the chimney among other parameters. Besides the temperature rise attainable, cost per unit height of the chimney, compactness and accessibility of the air exit point are of importance in this study. For instance, checking the air temperature of the air exiting the chimney through connected temperature probes will dictate the maximum height of the chimney that can be comfortably reached during experimentation.

Figure 2.10 shows another design of a solar chimney which varies from the design shown in Figure 2.9 in the way the solar radiation is trapped by the absorber plate. In the greenhouse type solar chimney, the glazing is a circular glazing profile while the

design shown in Figure 2.9 has a rectangular profile with only one face receiving the solar radiation.

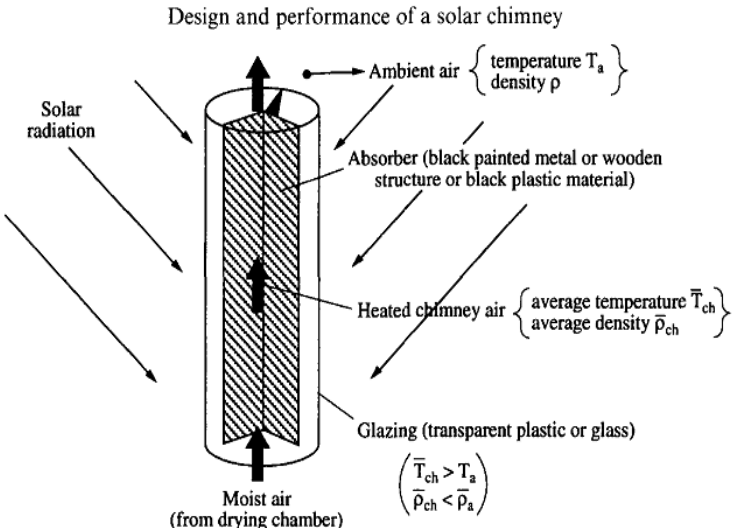

Figure 2.10: Greenhouse solar chimney (Ekechukwu and Norton, 1997)

By comparing the two designs of solar chimneys in Figures 2.9 and 2.10 having the same surface area and under the same test conditions, the design in Figure 2.10 could result in a much higher air temperature rise because of its surface ability to receive the solar radiation no matter the angle of the incident radiation.

Assuming glass is to be used for constructing the chimney unit, the circular profile greenhouse solar chimney (Figure 2.10) would prove to be more complex to construct than the rectangular profile flat-plate chimney in Figure 2.9. For this reason, this study considered the simpler profile, the rectangular design to suit needs of areas with low levels of skills such as Zambia.

In studies to construct a natural convection solar drying system, inexpensive and locally available materials have been used. Some of the materials used include; wood, glass, clear plastic, galvanised iron sheets, wire mesh, steel tubes (Grainger *et al.*, 1981; Esper *et al.*, 1989; Ekechukwu and Norton, 1999b; Simate, 2003). In these studies, the choice of material have been based majorly on; cost, availability, durability, level of skill required by a particular material, weight to volume ratio and the product to be dried. For the case of this study, the local availability, cost, and workability of the materials were considered as benchmarks for choosing the materials

for construction of the dryer. In the following section, a review of solar tunnel dryers is given.

2.6 Solar tunnel dryers

Solar tunnel dryers have a distinct collector unit that serves the purpose of heating air and a drying unit where the product is located. Figure 2.11 shows a forced convection solar tunnel dryer developed by Schirmer *et al.* (1996) and used to dry bananas.

The major parts of the dryer are labelled as: (4) solar collector unit covered with a clear plastic sheet, (7) drying tunnel covered with clear plastic where the product was placed for drying. Parts 1, and 3 were the fan and solar PV module respectively. Air was sucked in from the part labelled 2.

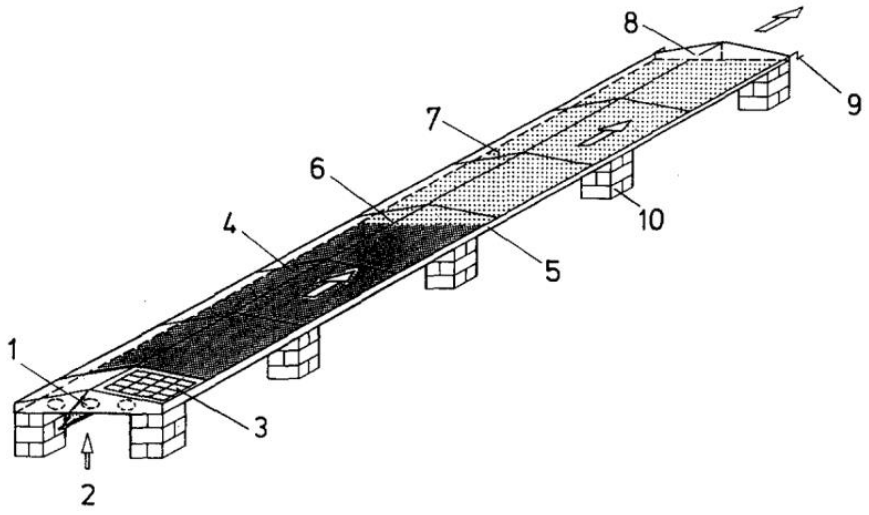

Figure 2.11: Solar tunnel dryer configuration

The results of the experiment in this type of a dryer indicated the varied collector temperatures of between 40 ^{o}C and 65 ^{o}C with global solar radiation of up to 1000 W/ m^2 respectively. Under these conditions, the bananas with an initial moisture content of 69 % (w.b.), were dried to a final moisture content of 30 % (w.b.) in 2-3 days. Though the dryer significantly reduced the moisture content; the drying time depended on the weather conditions, specifically the amount of insolation registered.

Hossain and Bala (2007) investigated the drying of chilli in a forced convection mixed-mode solar tunnel dryer shown in Figure 2.12, and the results indicated a reduction in drying time by over 10 hours as compared to OSD.

The moisture content of the chilli was reduced from 2.85 to 0.05 kg kg $^{-1}$ (d.b.) in 20 hours while OSD took 32 hours to bring down the moisture content to 0.4 kg kg $^{-1}$ (d.b.). Solar tunnel dryers therefore significantly reduce the drying time. In terms of physical quality, the final quality of the dried chilli from the solar dryer (Figure 2.11) was better compared to the open sun dried chilli because the solar tunnel dryer protected the chilli completely from dust, insects and any other foreign matter and this emphasises the benefits of solar dryers over OSD.

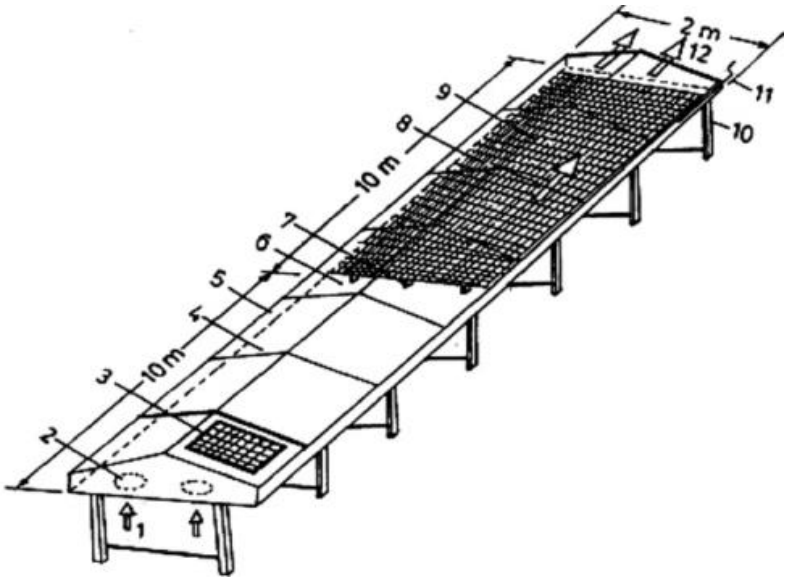

Figure 2.12: Forced convection mixed mode solar tunnel dryer used to dry hot chilli

The solar tunnel dryers shown in Figures 2.11 and 2.12 are similar in design with other solar tunnel dryers in various studies listed (Mastekbayeva *et al.*, 1999; Bala *et al.*, 2003; Hossain and Bala, 2007). The configuration of solar tunnel dryers where the solar collector and the drying tunnel are directly connected simplified the construction and reduced cost as first reported in Mastekbayeva *et al.* (1999).

It is therefore worthwhile to note that solar tunnel dryers among the many existing solar dryers provide a good option for developing countries with low incomes accompanied with shortage of skilled personnel.

2.7 Sizing of solar dryers

Solar dryers are constructed to dry a recommended amount of product per loading per time and this is known as the loading density (LD). It is a measure of the amount of

product loaded per unit tray area and the LD aids in sizing the drying area of the dryer. The LD is calculated mathematically according to Equation (2.4) (Leon *et al.*, 2002).

$$LD = \frac{W_{Fresh\,Product}}{A_d} \qquad (2.4)$$

Where; $W_{FreshProduct}$ is the weight of fresh product in kg, and A_d is the area of the drying chamber in m^2.

For mango, the product in this study, an LD of 2.6 kg/m^2 has been previously used (Akoy *et al.*, 2006). The interpretation of the LD is that for every square meter of drying area, a load of 2.6 kg of mango can be sufficiently loaded to dry. With a known LD, the drying unit area can be defined for a solar dryer. A unique feature of solar tunnel dryers is that the collector unit and the drying unit have the same size in terms of area. Therefore, by sizing the drying unit, the collector unit size is set automatically and this emphasizes the simplicity in construction of solar tunnel dryers.

2.8 Thin layer drying and mathematical modelling

The various studies of fruit and vegetable drying in solar drying have proceeded under thin layer drying. The product is sliced into small thicknesses and then dried (Belessiotis and Delyannis, 2011). This enhances the drying rate which is controlled by many factors including the size of the product and most importantly, use of thin layer mathematical models to predict drying rates is made possible. The mathematical models scope from; theoretical, semi-empirical and pure empirical (Madamba *et al.*, 1996; Midilli *et al.*, 2002). Theoretical models cater for only the internal resistance to moisture transfer while the semi-empirical and purely empirical models take into account the external resistance to moisture transfer to the air.

The focus of this study was on empirical thin layer models because of their associated advantages which include the ease of use despite a compromise in the theory and the non-requirement for assumptions of the geometry of the food, mass diffusivity and conductivity (Akpinar, 2006). However, the validity of empirical models is only limited to the temperature, relative humidity, air velocity and moisture contents in which they have been investigated (Akpinar, 2006). This suggests that empirical

models are site specific and may vary from product to product depending on the products moisture content.

Among the empirical models in literature are the Newton's model and Page model shown in Equations (2.5) and (2.6) respectively (Madamba *et al.,* 1996). The Newton's model which is analogous to the Newton's law of cooling is based on the assumption that the internal resistance to moisture movement to the surface of the product is negligible.

$$\frac{M - M_e}{M_O - M_e} = \exp(-kt) \tag{2.5}$$

$$\frac{M - M_e}{M_O - M_e} = \exp\left(-kt^N\right) \tag{2.6}$$

Where; t is the elapsed drying time in seconds or minutes or hours, M_o, M, M_e are the initial moisture content, moisture content at any time and equilibrium moisture content respectively, while k and N are the experimental model constants.

2.9 Closing Remarks

It can be pointed out that solar drying has a huge role in crop drying including fruits and vegetables due to its capability to maintain quality while reducing the drying time significantly. From the several classifications and designs of solar dryers in literature, active solar dryers are more common than natural convection dryers and this is attributable to better and controllable air flow rates in the active systems. However, natural convection systems which depend on buoyancy and wind pressure for air flow are less efficient in action. The advantages of natural convection systems are their low cost and ease of operation. Solar tunnel dryers, which can be made active or passive have one of the simplest configurations, hence easier to construct especially in areas with scarcity of skilled personnel. Through experimentation, several thin layer models have been developed to make possible prediction of the drying time among other parameters required. The ability to predict drying time is aimed at achieving a quality product and cost reduction by drying only for the appropriate time. The focus of this study was on experimental investigation of a natural convection solar tunnel fruit dryer.

CHAPTER THREE

3. MATERIALS AND METHODS

This chapter describes the materials and methods used in the study. For purposes of clarity, the chapter presents the methods and materials specific to each objective. The study site and the period in which the experiments were done have also been indicated.

3.1 To construct a natural convection solar tunnel dryer for experimentation

The design of solar tunnel dryers according to past studies have been described as simple, easy and cheap to construct (Schirmer *et al.*, 1996; Bala *et al.*, 2003; Hossain and Bala, 2007). For these reasons, this study adopted the general design from these past studies but with the incorporation of a solar chimney to make the dryer a natural convection type.

3.1.1 Determination of the dryer dimensions

i. From the literature review section (section 2.7), and using Equation (2.4), the area of the drying unit was determined for an LD for mangoes of 2.6 kg/m^2 (Akoy *et al.*, 2006). However, for experimental purposes and minimization of cost, a drying unit size slightly less than 1 m^2 was chosen as shown in Table 3.1

ii. By sizing the drying unit, the collector unit was defined automatically as solar dryers have a uniqueness of equal collector and drying unit dimensions as seen from chapter 2.

iii. Since the chimney unit is usually attached at one end of the drying unit, its width was defined by the width of the drying unit.

iv. To simplify the design and to keep the dryer as compact as possible for transportation purposes, and also to enable reaching the chimney exit in order to connect the temperature probes, the chimney was made square in shape, hence its height was equal to its width.

v. In summary, the loading unit was sized based on the LD of mangoes, and then the other units were subsequently sized. A summary of the major component units and their dimensions are shown in Table 3.1.

Table 3.1: Sizes of the different component units in the solar tunnel dryer

	Dryer unit	Length, m	Width, m	Height, m	Surface Area, m^2
1.	Drying unit	1.00	0.75	-	0.75
2.	Drying tray	0.96*	0.72*		0.69*
3.	Collector unit	1.00	0.75	-	0.75
4.	Chimney unit		0.75	0.75	0.56
4.	Dryer legs	0.02	0.02	0.60	

*Effective tray dimensions and area

More details of the component units of the dryer with their corresponding dimensions are shown in the construction drawings attached in Appendices II-VIII.

3.1.2 Material selection and the dryer construction

The materials for the construction of the dryer were chosen based on cost, the availability from the local stores and their suitability for use in a particular unit of the dryer. Appendix I shows the materials that were used with their respective costs.

After procurement of the chosen materials, the dryer was then fabricated from the Department of Agricultural Engineering workshop by following the construction drawings attached in Appendix II-VIII. The photographs of the fabricated solar tunnel dryer are shown in Figures 3.1 and 3.2.

Figure 3.1: Side view of the solar tunnel dryer

Figure 3.2: End view of the solar tunnel dryer

3.1.3 Description of the dryer and its components

The fabricated solar tunnel dryer shown in Figures 3.1 and 3.2 consists of three major components: the collector unit, the drying unit, and a bare flat-plate chimney unit. Each of the units has been described in detail in the following sections.

3.1.3.1 The collector unit

The solar collector unit was a flat-plate type with air flow above the absorber plate while the cover was a transparent 200 μm polythene sheet. The reason for using this type of collector unit is because of their low thermal losses (Brenndorfer *et al.*, 1987; Ekechukwu and Norton, 1999b). The absorber plate was made from Galvanized Iron (GI) sheet and in order to increase the solar absorptivity of the absorber plate, it was painted black using mat black paint. To minimize heat losses to the surrounding, the base and sides of the collector unit were insulated with 20 mm Styrofoam sheets. The overall dimensions of the collector unit were 1.0 m × 0.75 m (L× W) as shown previously in Table 3.1.

3.1.3.2 The drying unit

The drying unit, adjacent to the collector unit was made from the same materials as the collector unit and in the same configuration as the collector unit. The base and sides of the drying unit were also clad with 20 mm Styrofoam sheets to minimize heat losses to the ambient air. To provide for the drying of the product, the drying unit was mounted with a removable wire mesh tray to hold the product during the drying as shown in Figure 3.3. The overall dimensions of the drying unit were 1.0 m× 0.75 m (L× W) while the tray had an effective area of 0.69 m^2. The end of the dryer unit was mounted with a vertical bare flat-plate chimney described in the following section.

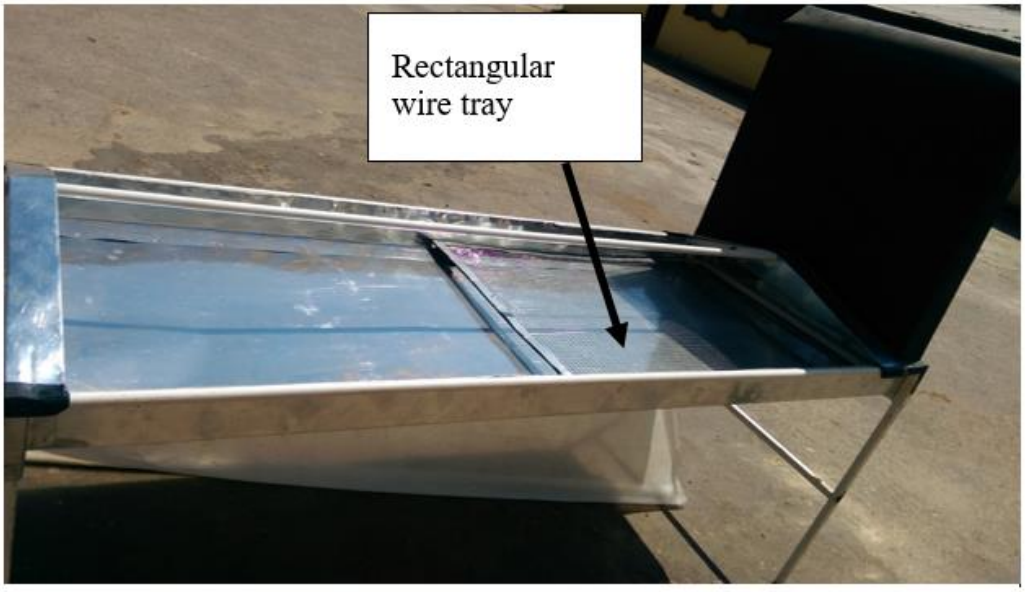

Figure 3.3: Solar tunnel dryer showing the product drying unit mounted with a rectangular tray

3.1.3.3 The chimney unit

The chimney unit which serves the purpose of reheating the air exiting the drying unit was a bare flat-plate type collector. The solar radiation receiving surface of the chimney was painted black with mat black paint to absorb as much of the incident solar radiation as possible during operation. The dimensions of the chimney were 0.75 m × 0.75 m (L× W) with an air channel of 0.1 m. It was constructed from 0.3 mm thick GI sheet and was mounted vertically adjacent to the drying unit in a North-South orientation. The dryer was supported by four dryer legs 0.6 m above the ground and all the units were detachable to allow for easy assembly and re-assembly for transportation purposes.

3.1.4 Mode of operation of the dryer

The mode of operation of the dryer showing the air flow is given in Figure 3.4. As illustrated in the figure, a unidirectional air flow was assumed. The solar radiation falling through the transparent cover in both the drying and collector units heats the air entering the collector unit through convective transfer at the cover and the absorber plate.

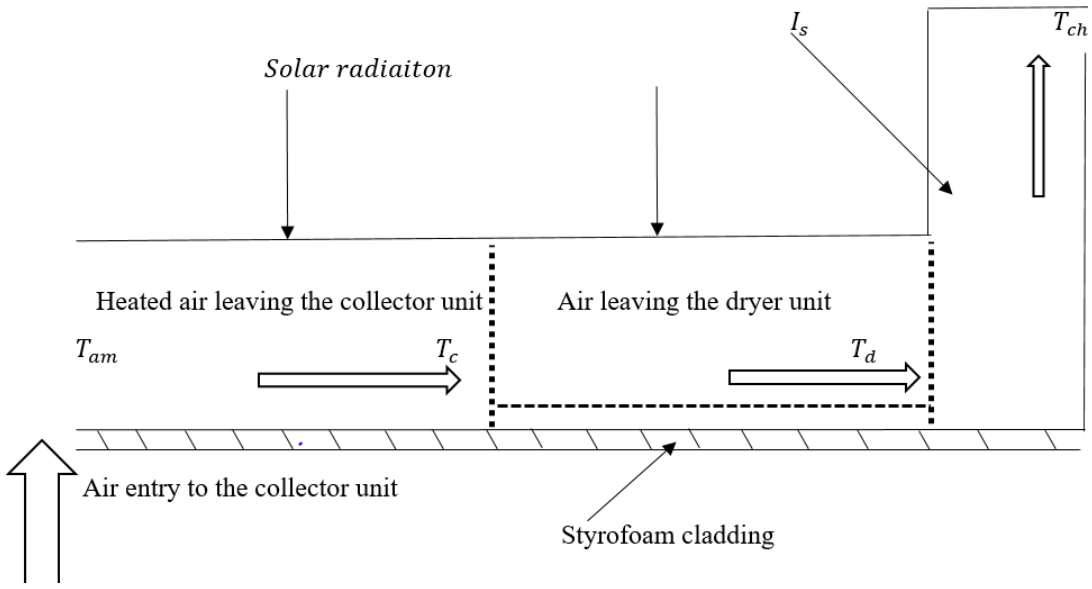

Figure 3.4: Air flow in the solar tunnel dryer

The heated air becomes less dense compared to ambient air and as a result, buoyancy pressure is generated due to the density differences between the air inside the dryer and ambient air. The buoyancy pressure together with the wind force causes the air in the collector unit to be displaced to the drying unit.

At the drying unit, if the product is loaded, mass and heat transfer between the product and the air occurs and hence the air temperature is expected to reduce while the relative humidity increases. The heat and mass transfer process which occurs simultaneously causes the product to dry with time. In addition to drying caused by the heated air, the solar radiation through the transparent cover of the drying unit facilitates the product to be dried directly. Therefore in the solar tunnel dryer, the product is dried through convective heat transfer and direct heating and this results in high drying rates.

With no product loaded in the drying unit, the air from the collector unit continues to be heated as it passes through the drying unit and therefore becomes hotter than the air at the collector unit. Through the chimney unit, the air exiting the drying unit is further heated and rises by natural convection to the outside and the cycle repeats again as long as there is solar radiation.

3.2 To determine an appropriate mathematical thin layer model to predict the drying characteristics of mango and validate it against experimental results

The first experiments were carried out under no load, that is to say, no mango was loaded in the drying chamber. The no load experiments have been referred hereafter as dry run experiments. The dry run experiments were then followed by the mango drying experiments. From the moisture content results of mango, an appropriate thin layer model which best predicts the drying of the product under the observed conditions was obtained and validated against experimental results.

3.2.1 Description of the study area

The experiments were carried out at the Department of Agricultural Engineering field station at the University Zambia with coordinates; Latitude 15.3°S; Longitude 28.3°E. The solar tunnel dryer was positioned on an open flat ground surface outside the University of Zambia, Department of Agricultural Engineering field workshop under natural conditions during the experiments. Figure 3.5 illustrates the experimental set-up.

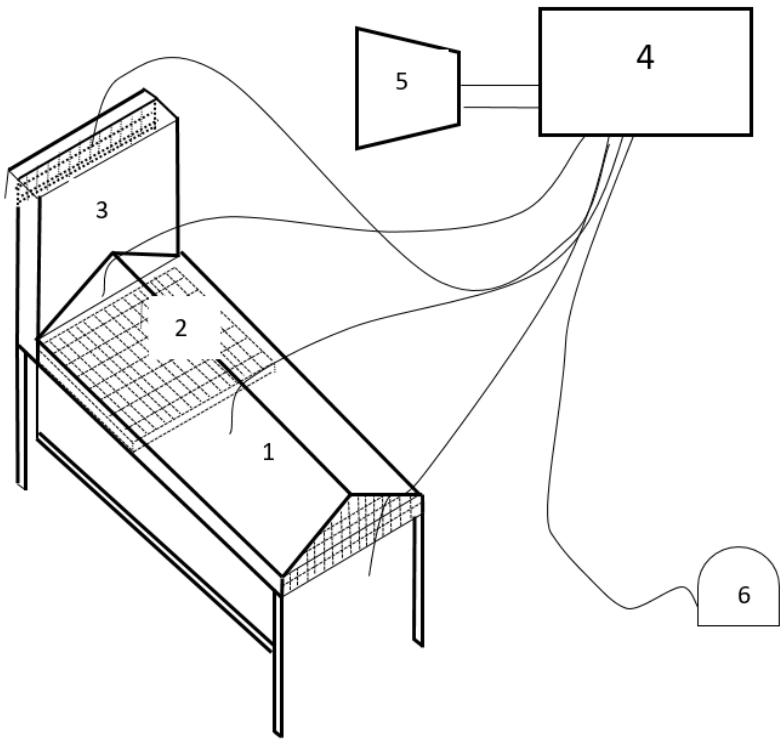

Figure 3.5: Experimental set-up of the solar tunnel dryer and the equipment: (1) collector unit, (2) drying unit, (3) bare flat- plate chimney Unit, (4) Data logger (5) Computer and (6) solar pyranometer

A multi probe Campbell Scientific Inc data logger (4) (model: CR 1000) was connected to the solar tunnel dryer to record the air temperatures, relative humidity and solar radiation. The data logger recorded the air temperatures through thermocouple type temperature probes (model: 108 – L and accuracy of ±0.01 ºC). The temperature probes were capable of recording temperature ranging between -5 and +95 ºC.

The relative humidity was recorded using a relative a humidity probe (model: HMP60-L) that was capable of temperature and humidity ranges of -40 ºC to 60 ºC and 0 and 100 % respectively, whereas the solar insolation was recorded by a pyranometer (model: CMP6-L) placed on a flat horizontal ground surface near the solar tunnel dryer. Finally, the air velocity was measured at its entry to the collector unit (V_{am}) and inside the collector unit (V_c) using a digital air flow meter (model: TES 1340) that had an accuracy ± 0.01 m s^{-1} for air velocities between 0 and 30 m s^{-1}.

The air temperatures were recorded at the following points: entry to the collector unit, exit of the collector unit, exit of the drying unit and at the exit of the chimney unit. At these points, the ambient air temperature (T_{am}), the collector air exit temperature (T_c),

the drying unit air exit temperature (T_d) and the chimney air exit temperature (T_{ch}) were recorded respectively using connected temperature probes. The air relative humidity at the following points were recorded; the entry point to the collector (RH_{am}), collector unit exit (RH_c), and the drying unit exit (RH_d). These recorded air conditions vary with time of the day and they define the drying of the product.

3.2.2 Dry run experiments

These experiments were conducted between the months of October and November to investigate the performance of the dryer prior to drying the product and to help inform any adjustments to the dryer geometry if found necessary. The parameters of interest during the dry run experiments were; attainable air temperatures in the dryer, ambient relative humidity reduction and air flow direction under solar insolation typical of the study area. The dry run experiments were conducted according to the description in steps i to iii.

i. The dryer and the equipment were arranged as illustrated in the experimental set-up in Figure 3.5 and the experiments conducted between 09:00 h and 16:00 h due to the abundance of the solar radiation in this period of the day.
ii. Through the data logger, the air temperatures (T_c, T_d, T_{ch} and T_{am}), the relative humidity (RH_c, RH_d, and RH_{am}) and the solar insolation were recorded every minute and stored in the computer.
iii. The air velocities V_{am} and V_c were measured using the air flow meter in hourly intervals during the experimental period.

After the dry run experiments, the initial moisture content of mango was determined followed by the mango drying experiments in the solar tunnel dryer under natural conditions as described in the next sections.

3.2.3 Determination of the initial moisture content of mango

The procedure described below was followed to determine the initial moisture content (M_o) of mango.

i. Ripe mango whose degree of ripeness was not determined experimentally but based on the fact that it was ready and acceptable for consumption by the consumers was purchased locally from the markets

ii. The purchased mango was then cleaned using clean tap water for food safety concerns and for final good quality of the dried product

iii. Using the standard method of moisture content determination (AOAC, 2005) described in steps (iv) – (ix) the initial moisture content was determined

iv. Mango was peeled and sliced into approximately 3 mm thickness using a table knife

v. A clean empty petri dish with known weight was loaded into an oven at 105 °C for 3 h and left to cool

vi. The sliced mango was put into the petri dish in (v) and 10 g was weighed from a digital weighing balance (model: PE 3000, accuracy, ±0.1 g). The weight of the dish and sample was recorded as W_1.

vii. The dish and sample were then loaded into the oven and left to dry for 3 h at 105 °C

viii. At the end of the 3 h, the sample in the petri dish was left to cool and then reweighed for the final dry weight (W_2)

ix. Using Equation (3.1)., the initial moisture content was calculated in wet basis (w.b.)

$$M_O = \frac{(W_1 - W_2)}{W_1} \times 100 \qquad (3.1)$$

3.2.4 Procedure of the mango drying experiments

i. For each experimental set, ripe mango was purchased from the market on an evening before the day of the experiment and kept under room temperature overnight

ii. Starting at 07:00 h on the day of the experiment, mango was cleaned, peeled and sliced into approximately 5 mm thickness (Akpinar, 2006)

iii. Three 100 g samples were weighed from the sliced mango using a digital weighing balance and placed onto 3 square polyethylene nets for the purpose of loading in the drying unit and unloading the samples during weight loss measurements

iv. The square nets containing the mango slices were then loaded into the wire tray located in the drying unit

v. The rest of the drying tray area which was covered by a similar square net as in step iii was spread with a thin layer of sliced mango as shown in Figure 3.6. At

full capacity, the drying unit could carry up to 1.8 kg of sliced mango, hence a LD of 2.6 kg/m^2.

Figure 3.6: Loading the solar tunnel dryer with the sliced mango

vi. At 09:00 h, the set-up of the equipment and preparation of the product was complete and the drying of the product started. Through the data logger, air temperatures, T_d, T_{ch} and T_{am}, relative humidity RH_c, RH_d, and RH_{am} and finally, the solar insolation were recorded as the drying progressed until the end of the experimental day (16: 00 h)

vii. To track the moisture loss from the samples, weight loss was taken every 30 minutes in the first 6 h of drying and then hourly after the 6^{th} hour until there was no significant change in the weight of the samples in successive weight measurements

viii. The weight loss measurements were taken by unloading the square nets containing the three samples and weighing on the digital balance. The process of weight loss measurement took approximately 60 seconds each time it was done

ix. From the weight loss measurements, the moisture content was calculated using Equation (3.2)

$$M = 100 - \left(\frac{W_1(100 - M_O)}{W_2} \right) \qquad (3.2)$$

Where; M is the moisture content (w.b.) at any time, W_1 is the initial weight of the sample and W_2 is the weight of the sample during the weight loss measurement

x. At the end of a drying day, if the mango was still losing weight, it was packed tightly in a polyethylene bag and stored under room temperature to prevent any moisture migration in and out of the product during the night

xi. Drying was resumed the following day by unpacking the mango from the polythene bag and reloading into the dryer

3.2.5 Simple Linear Regression

This was done to investigate the relationship between the dependent variable, collector temperature rise above ambient attained at the collector unit and the independent variable, solar insolation. The aim of carrying out the regression analysis was to be able to predict the variation of drying air temperature under varying solar insolation. The following procedure was followed (Statisticssolutions.com, 2016).

i. The difference between collector air temperatures T_c and ambient air temperature T_{am} was calculated from the experimental values and noted as T_c-T_{am}.

ii. The difference T_c-T_{am} in step (i) and their corresponding recorded solar insolation were plotted in scatter. In the scatter plot, the solar insolation was on the x- axis (independent variable) and T_c-T_{am} on the y-axis (dependent variable).

iii. Finally, the line of best fit, the equation and the regression coefficient R^2 were obtained.

3.2.6 Thin layer modelling of the drying curve

From the moisture content results, the moisture ratio (MR) which is mostly defined according to Equation (3.3) was calculated. However, for solar tunnel dryers, a simplified form described by Equation (3.4) was used to calculate the MR (Pala *et al.*, 1996; Doymaz, 2004; Goyal *et al.*, 2006). The reason given for the simplification is that in solar tunnel dryers, the samples being dried are subjected to a varying temperature and relative humidity along the length of the tunnel.

$$MR = \frac{M - M_e}{M_o - M_e} \tag{3.3}$$

$$MR = \frac{M}{M_o} \tag{3.4}$$

Where; M and M_e are the moisture contents (w.b.) at time t during the drying and at equilibrium respectively.

The MR results from Equation (3.4) were fitted into 12 empirical thin layer models as shown in Table 3.2 using the Matlab R2011b curve fitting tool (*cftool*) to determine an appropriate thin layer model for mango. The *cftool* requires a maximum of three input parameters and include the X data, Y data and Z data. The Matlab *cftool* was chosen because of its simplicity and also the robust capabilities of Matlab such as producing good quality graphics although other curve fitting tools exist for example curve expert etc. Figure 3.7 illustrates the user interface and the data fitting process using the *cftool*.

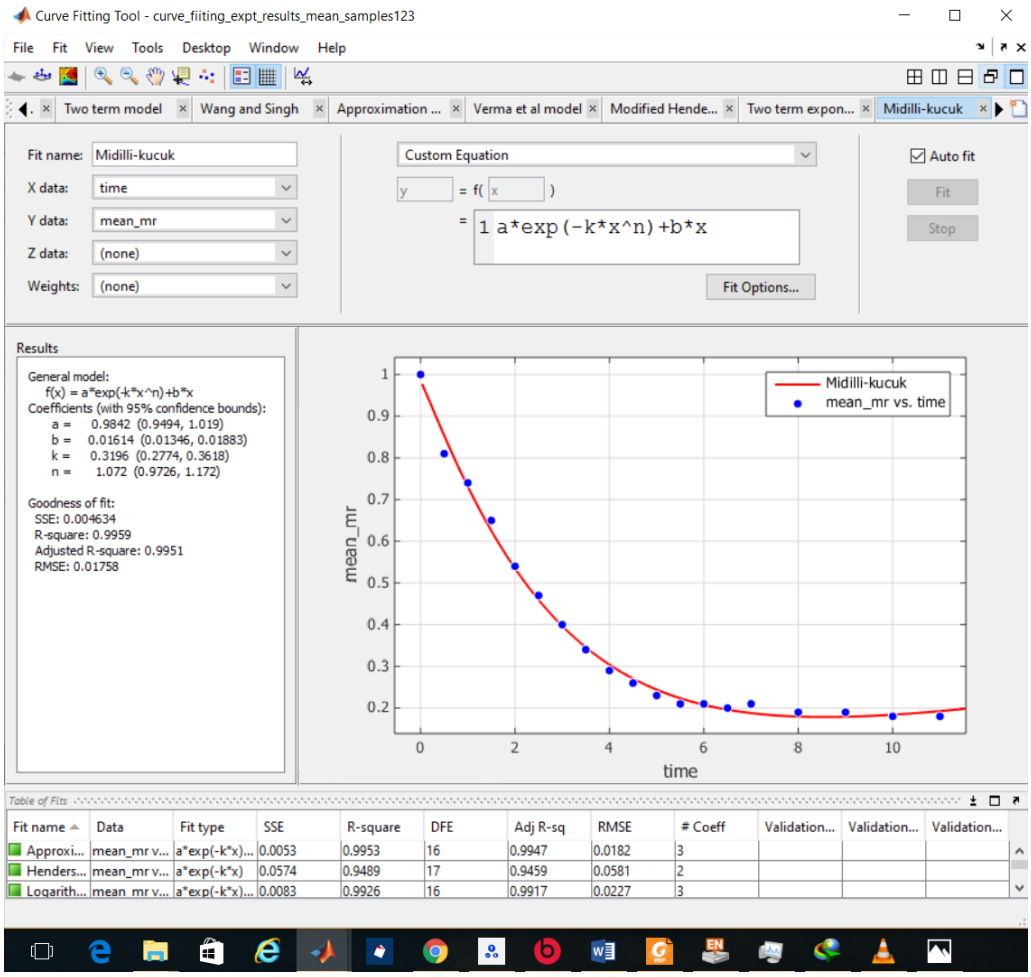

Figure 3.7: Matlab cftool interface and data fitting

In Figure 3.7, the input parameters were the drying time on the X data field and MR on the Ydata field. This was followed by entering the model equations for example, the Midilli-Kucuk model is; $MR = aexp(-kt^n)+bt$. Once the parameters were entered,

the tool determined the constants *a, b, k and n* and the statistical parameters SSE, RMSE and r^2 and subsequently plotted the predicted MR and experimental MR as depicted in Figure 3.7. These process was done for all the models shown in Table 3.2.

Table 3.2: Thin layer models

Model no.	Model Name	Model Equations
1.	Newton	$MR = exp(-kt)$
2.	Page	$MR = exp(-kt^n)$
3.	Modified Page	$MR = exp[-(kt)]^n$
4.	Hederson and Pabis	$MR = aexp(-kt)$
5.	Logarithmic	$MR = a\,exp(-kt) + c$
6.	Two term	$MR = a\,exp(-kt) + c$
7.	Approximation of Diffusion	$MR = a\,exp(-kt) + (1-a)exp(-kbt$
8.	Verma et al.	$MR = a\,exp(-kt) + (1-a)exp(-gt$
9.	Modified Henderson and Pabis	$MR = a\,exp(-kt) + b\,exp(-gt) + c\,exp(-ht)$
10.	Two term exponential	$MR = a\,exp(-kt) + (1-a)exp(-kat)$
11.	Wang and Singh	$MR = 1 + at + bt^2$
12.	Midilli-kucuk	$MR = a\,exp(-kt^n) + bt$

Source: (Akpinar, 2006)

The best model was established based on the criteria of three statistical parameters: the Sum of Square Error (SSE), coefficient of determination (r^2) and Root Mean Square Error (RMSE) that are calculated by the *cftool* according to Equations (3.5), (3.6) and (3.7) respectively.

$$SSE = \sum_{i=1}^{n} w_i \left(MR_{Exp} - MR_{\Pr ed}\right)^2 \tag{3.5}$$

$$r^2 = 1 - \frac{SSE}{\sum_{i=1}^{n} w_i \left(MR_{Exp} - \overline{MR}_{Exp}\right)^2} \tag{3.6}$$

$$RMSE = \sqrt{\left(\frac{SSE}{v}\right)} \tag{3.7}$$

After establishing the appropriate thin layer model, the model was used to predict the MR and the model predicted MR compared with the experimental MR in order to validate the model.

3.3 Dryer performance evaluation

From the attained conditions in the dryer, the three major units namely; the collector unit, the drying unit and the chimney unit were analysed for their performance as detailed in the following section.

3.3.1 The collector unit efficiency

The collector unit was analysed for its performance by obtaining the collector efficiency which expresses the heat gained as a ratio of the solar insolation falling on its surface. The collector unit efficiency was calculated using Equation (3.8) (Ahmad *et al.*, 1996; Weiss and Buchinger, 2012)

$$\eta_c = \frac{\dot{m}C_p\Delta T}{A_c I_s} = \frac{\dot{m}C_p\left(T_c - T_{am}\right)}{A_c I_s} \tag{3.8}$$

Where; η_c is the collector efficiency, $\dot{m}$ is the air mass flow rate in kg/m^{2}s, C_p is the specific heat capacity of the air in J/kg K, A_c is the area of the collector in m^2 and I_s is the solar insolation in W/m^2.

3.3.2 The drying efficiency and pick-up efficiency

In the drying unit, two parameters were evaluated i.e. the drying efficiency and the pick-up efficiency.

The drying efficiency was calculated using Equation (3.9) used for natural convection dryers (Mastekbayeva *et al.*, 1998).

$$\eta_{drying} = \frac{WL}{I_{ST}A_c} \tag{3.9}$$

Where; η_{drying} is the drying efficiency, W is the total moisture removed in kg, L is the latent heat of vaporization of water at the dryer air temperature in J/kg and I_{ST} is the total solar insolation registered for the drying time.

The pick-up efficiency is a parameter that defines the utilized capacity of the heated air in evaporating the moisture from the product. The pick-up efficiency was calculated according to Equation (3.10) (Brenndorfer *et al.*, 1987).

$$\eta_{pick-up} = \frac{h_d - h_c}{h_{as} - h_c} \tag{3.10}$$

Where; $\eta_{pick-up}$ is the pick-up efficiency, h_d is the absolute humidity of the air leaving the drying unit in kg/kg, h_c is the absolute humidity of the air leaving the collector unit and entering the drying unit in kg/kg and h_{as} is the adiabatic saturation humidity of the air entering the drying unit, kg/kg.

To find the absolute humidity, the air temperature and relative humidity attained in the dryer were used to read the absolute humidity from the psychrometric chart.

3.3.3 The chimney unit buoyancy pressure head

The chimney unit was evaluated for the developed buoyancy pressure head developed. The buoyancy pressure head generated by the chimney can be calculated according to Equation (3.11) (Brenndorfer *et al.*, 1987).

$$\Delta P_b = gH\left(\rho_{am} - \bar{\rho}_{ch}\right) \tag{3.11}$$

Where; ΔP_b is the chimney buoyancy pressure head in N m^{-2}, g is the acceleration due to gravity in m s^{-2}, H is the chimney height in m, ρ_{am} is the ambient air density in kg m^{-3} and $\bar{\rho}_{ch}$ is the mean chimney air density in kg m^{-3}.

Between air temperatures of 25 and 90 °C, Equation (3.11) was manipulated to yield Equation (3.12) which uses the air temperatures as opposed to Equation (3.11) which uses air density to calculate buoyancy pressure (Brenndorfer *et al.*, 1987).

$$\Delta P_b = 0.00308gH\left(T_{ch} - T_{am}\right) \tag{3.12}$$

By using Equation (3.12), the buoyancy pressure head was obtained using the temperature of the air leaving the chimney unit and ambient air temperature defined earlier as T_{ch} and T_{am} respectively.

3.4 Closing remarks

In this chapter, the materials and methods specific to each objective were presented. The study area and the period in which the study was conducted have been indicated. A number of tools and materials used to carry out the study have also been mentioned and include among others a data logger, a digital weighing balance, an oven, Matlab *cftool* etc. Photographs have been used as much as possible to communicate the experimental procedures as they carry more clarity than words and finally, equations used for evaluating the dryer performance have been described and presented.

CHAPTER FOUR

4. RESULTS AND DISCUSSIONS

This chapter presents the results and discussions of the study. The chapter covers the following in detail; the dry run experiments, the mango drying experiments, thin layer modelling and finally the dryer performance evaluation plus some closing remarks.

4.1 Dry run results

A total of five dry run experiments were conducted in the constructed solar tunnel dryer and from these experiments, the first three were carried out with the air entry point located at the collector unit having no air guide as shown in Figure 4.1. From this configuration, the air entry into the collector unit was directly through the rectangular woven wire which served the purpose of blocking any large foreign particles and insects that might be carried by the air entering the dryer.

Figure 4.1: Solar tunnel dryer without an air guide

The air velocities V_{am} and V_c measured averaged between 0.36 m s^{-1} and 0.04 m s^{-1} respectively. With these relatively low air velocities, an undesirable air flow which can be described as bidirectional according to this study was experienced. This bidirectional air flow was evidenced from the recorded air temperatures at the collector entry, collector exit, drying unit exit and chimney exit abbreviated previously as T_{am}, T_c, $T_{d,\ and}T_{ch}$ respectively. These air temperatures are plotted in Figure 4.2.

From the desired air flow pattern which can be described as unidirectional referring to air entry from the collector unit and exit through the chimney unit, air was expected to get progressively hotter. However this was not the case (as seen from Figure 4.2) and this was attributed to an undesirable air exit from the collector entry point.

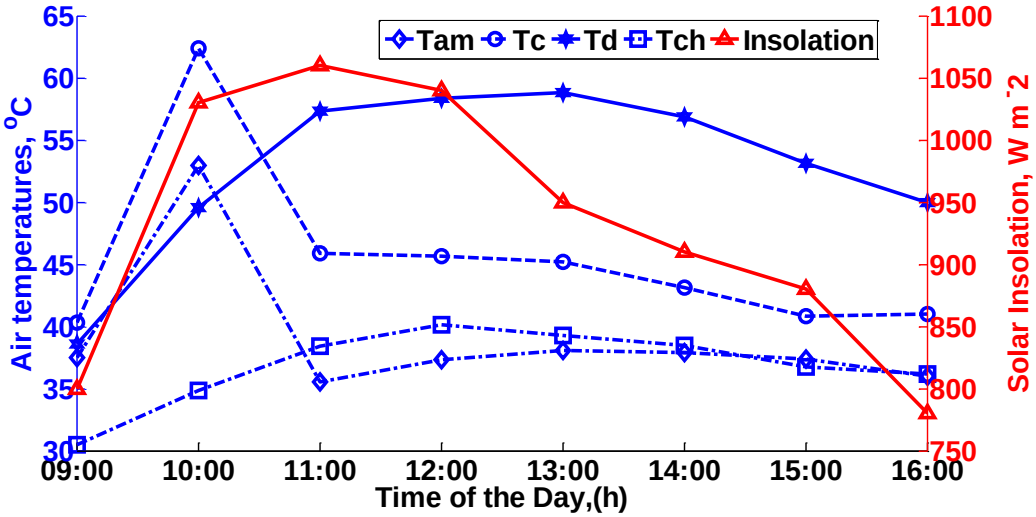

Figure 4.2: Recorded air temperatures and solar insolation with no air guide at entry

From Figure 4.2, the observed pattern of the air temperatures shows a complete distortion in the air flow. Between 09:00 h and 10:00 h, the air temperature T_c was higher than the air temperatures in all the other measured points and this was contrary to the results that would be expected for a unidirectional air flow under no load conditions. In a unidirectional air flow, air is heated progressively from the collector unit then at the drying unit and finally at the chimney unit and therefore, T_c should be less than T_d and T_d should be less than T_{ch}. Between 10:00 h and 11:00 h, a sharp drop in the air temperatures T_{am} and T_c is observed amidst increasing solar insolation while the air temperatures T_d and T_{ch} continued to rise. This suggested two relationships in the air temperatures which were; relationship between T_{am} and T_c and relationship between T_d and T_{ch} under the registered average solar insolation of 930 W m $^{-2}$.

These data suggest that there was some hot air mixing with cold air at the entry and exit points. The result of which was that the recorded mean ambient air temperature of 39.1 °C at the collector entry point was greater than the recorded chimney exit temperature of 36.8 °C. With these conditions and from Equation (3.12), it was deduced that the buoyancy pressure was negative or in other words, the chimney air flow in the chimney was in the reverse direction (Ekechukwu and Norton, 1997).

From the air temperatures observed in Figure 4.2, the identified relationships and the computed mean temperatures a conclusion was reached that air was entering into the dryer from the collector which was desirable and there was an undesirable entry from

chimney exit known as reverse flow (Ekechukwu and Norton, 1997). This was attributed to the configuration of the air entry point which was directly adjacent to the collector unit and was a woven square mesh to block relatively large foreign material from entering the dryer. With the possible cause of the anomalous bidirectional air flow identified, an air guide at the entry unit was incorporated in order to rectify the situation (see Figure 4.3) and the last two dry run experiments were conducted using this configuration.

Figure 4.3: Solar tunnel dryer with an incorporated air guide

With the air guide in place, the air flow in to the collector unit was confined to a perpendicular entry as shown in Figure 4.3 relative to the horizontal axis of the collector unit. The results of the air temperatures with the air guide in place showed a unidirectional air flow as shown in Figure 4.4 and from their average values. The average temperature values for $T_{am,}$ T_c, T_d, and T_{ch}, were obtained as 32.6 °C, 49.2 °C,

52.5 °C and 40.4 °C respectively and these were expected as the pattern described a flow from the collector entry point and exit at the chimney unit.

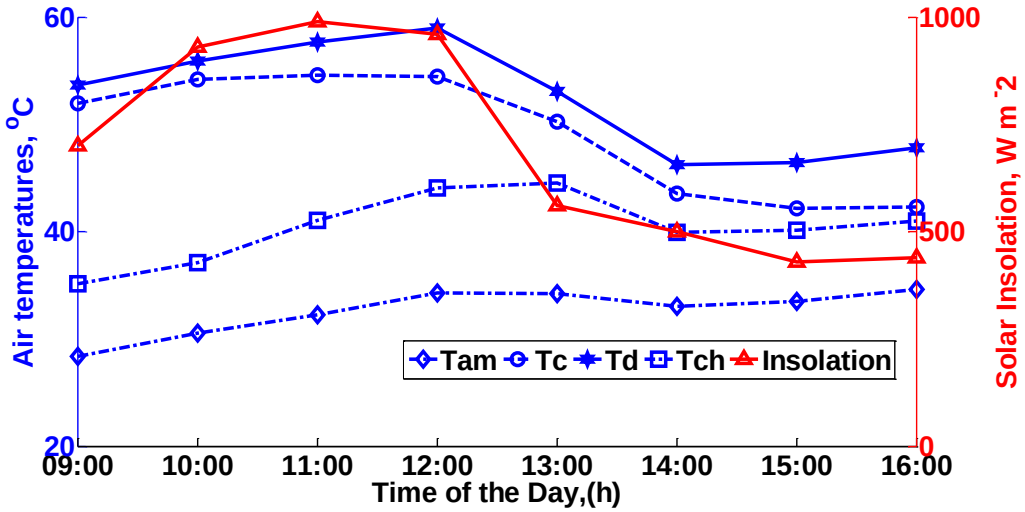

Figure 4.4: Air temperatures with air guide in place

From the pattern of variation of air temperatures observed in Figure 4.4 and the calculated average temperature values, it was clear that the air entering the collector unit was continually heated until the drying unit exit and this described a unidirectional air flow pattern. After the drying unit, a temperature drop of 8.8 °C from the drying unit temperature was observed at the bare flat-plate chimney exit. This drop in air temperature at the chimney exit was unexpected because the chimney unit, a bare flat-plate solar collector, was expected to continue heating the air from the drying unit to a higher temperature than the drying unit air temperature i.e. T_{ch} should be greater than T_d. This phenomenon of drop in temperature at the chimney unit could be explained by the high thermal heat losses associated with a bare-flat plate collectors (Ekechukwu and Norton, 1997).

The air relative humidity associated with the air temperatures in Figure 4.4 are shown in Figure 4.5. It is noticed that the relative humidity RH_{am}, RH_c and RH_d decreased appreciably from 30 % at 09:00 h to values as low as 6 % at 12:00 h while the solar insolation increased sharply to a peak value of 990 W m^{-2} in this time period. After 12:00 h a sharp decline in the solar radiation to a value of 440 W m^{-2} at 16:00 h was due to a cloud cover that was observed during this period. Within the recorded solar

insolation, the ambient relative humidity was reduced to average values of 6.4 % and 5.4 % for RH_c and RH_d respectively.

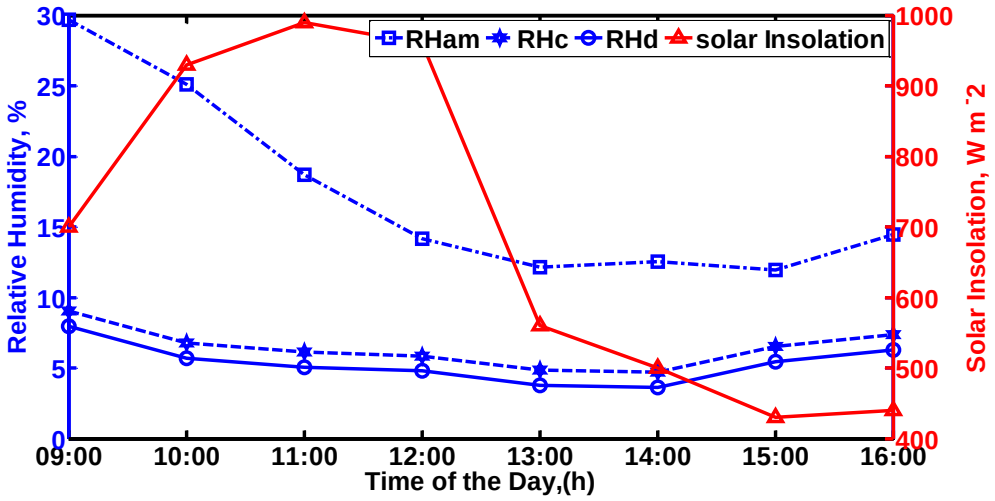

Figure 4.5: Dry run relative humidity and solar insolation with the air guide in place

At this point, it is worthwhile noting that the sharp increase in the solar insolation produced a corresponding decrease in the relative humidity thus pointing out a dependence of the relative humidity on the solar insolation. Despite the low air velocities of 0.36 m s^{-1} and 0.04 m s^{-1} for V_{am} and V_c respectively, the pattern of air temperatures and relative humidity shown in Figures 4.4 and 4.5 respectively, indicated that a unidirectional air flow was achieved with the air guide in place.

With a unidirectional flow achieved and the observed good conditioning of the ambient air by the dryer (Figure 4.5), the mango drying experiments were done with the dryer having a modified air entry.

4.2 To determine an appropriate mathematical thin layer model to predict the drying characteristics of mango and to validate it against experimental results

4.2.1 Initial moisture content and drying experiments

The initial moisture content of mango was found to be 80 % (w.b.) and this value is comparable to initial moisture contents obtained by Touré and Kibangu-Nkembo (2004) of 84 % (w.b.) and Ajila *et al.* (2007) of 81 % (w.b.). Following the initial

moisture content determination of mango, a total of 4 sets of mango solar drying experiments were carried out in the solar tunnel dryer.

The initial moisture content was reduced to final moisture contents of between 13 and 14 % (w.b.) in 11 hours in all the four experiments. After reaching the final moisture contents of between 13-14 % (w.b.), any further drying resulted in no further weight loss, hence moisture contents of between 13 and 14 % (w.b.) were considered as the equilibrium moisture contents under the air conditions in the drying unit.

The reduction in the initial moisture content to the final moisture contents is shown in the mango drying curve in Figure 4.6.

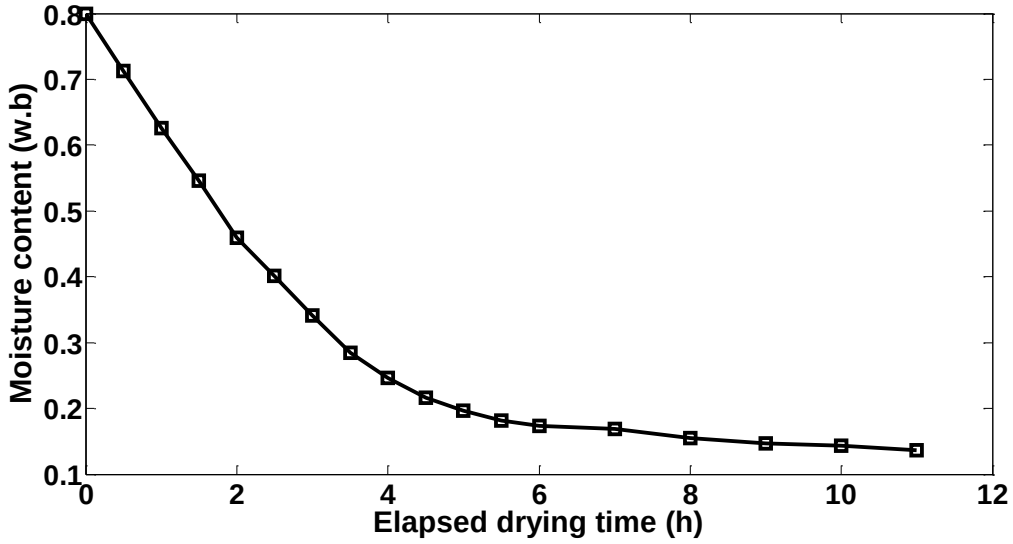

Figure 4.6: Mango drying curve

It can be observed from Figure 4.6 that the moisture content of the mango decreased continuously with time and hence drying took place in the falling rate period. The total drying time of 11 hours to the final moisture contents required one a half days of drying hence, 0 to 7 hours comprise the first day of drying because a typical experimental day was between 09:00 hours and 16:00 hours (7 hour period). The product was then kept in tight polyethylene bags overnight after the first day of drying under room temperature to prevent any moisture loss and gain to the atmosphere and then dried for the last 4 hours on a following day.

The final moisture contents of the dried mango in this study compare well with what has been reported previously (Dissa *et al.*, 2009; Goyal *et al.*, 2006) of 13.79 % (w.b.)

and 12 % (d.b.) respectively. Under these moisture contents, the product can be kept or packaged for sufficient periods of time because less water inform of moisture is available for microbial activity responsible for spoilage. In this way, dried products maintain a good keeping product quality acceptable for human consumption for reasonable periods of time.

The variations of the air conditions under which the mango was dried in the dryer are shown in Figures 4.7 and 4.8 for air temperature and relative humidity respectively.

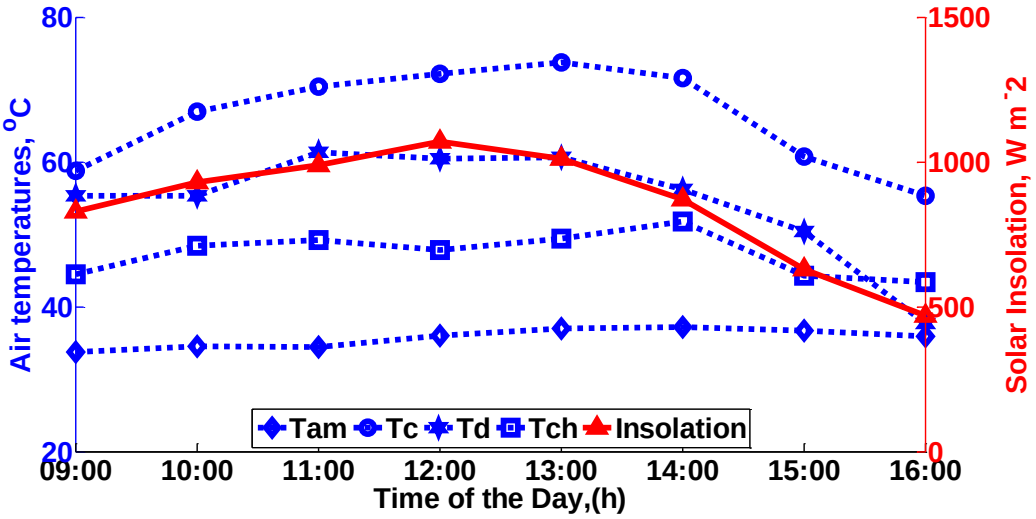

Figure 4.7: Air temperatures during mango drying experiments

With the solar insolation varying between a minimum of 470 W m^{-2} and a maximum of 1070 W m^{-2} as shown in Figure 4.7, the resulting pattern of dryer air temperatures shows that T_c was greater than T_d, T_{ch} and T_{am}. A maximum air temperature of 73.76 °C was recorded at the collector unit while the product was loaded in the drying unit. In the dry run air temperatures discussed in section 4.1, the maximum air temperature occurred in the drying unit.

The difference in the point where the maximum air tempeature occurs along the dryer between the dry run and product drying experiments is due to the heat mass transfer process during which the heated air temperature T_c picked up moisture from the product and resulted in; heat loss from the air to the product and moiture from the product to the air (drying process). The drying process resulted in a drop in air temperature from T_c to T_d of over 10 °C.

Despite the drop which was expected due to the heat and mass transfer processes, the air temperatures in the drying unit remained well above ambient by over 10 °C through out the day. A further drop in T_d to T_{ch} by an average value of 7.3 °C at the chimney unit was registered although T_{ch} remained above T_{am} by 7.7 °C. The ability of the chimney to keep the air temperature above ambeint was desirable for the generation of buoyancy pressure head which is discused in section 4.3.4. The relative humidities associated with the air temperatures in Figure 4.7 are shown in Figure 4.8.

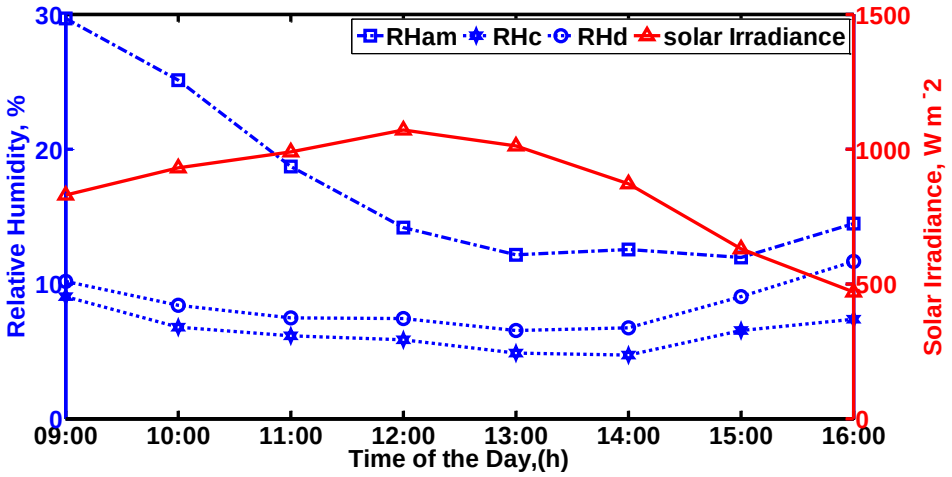

Figure 4.8: Relative humidity and solar irradiance during mango drying experiments

The ambient relative humidity varied between a minimum of 10 % and a maximum of 30 % and was lowered by over 50 % at the collector unit as shown in Figure 4.8. As observed for the air temperatures, the relative humidity exhibited a dependence on the solar insolation. The RH_{am}, RH_d and RH_c were lowest at around 13:00 hours and remained fairly low until 15:00 hours when a small increase was observed due to the decrease in the solar insolation. Therefore the relative humidity followed a diurnal regime defined by the solar insolation as reported by other authors (Pangavhane *et al.*, 2002). At the drying unit where the air picks up moisture from the product, the RH_d rose above the RH_c, but was below RH_{am}. The average relative humidity values were 17.3 %, 6.5 % and 8.4 % for $RH_{am,}$ RH_c and RH_d respectively. It can be seen from these values that the relative humidity of the air leaving the drying unit (8.4 %) was still relatively low compared to ambient (17.3 %) and could still be used sufficiently for drying.

The temperatures of the air from the dry run experiments and the mango drying experiments showed that there was a dependence of the air temperatures attained in the dryer on the solar insolation. The dependance of air temperatures on solar insolation was investigated using simple linear regression analysis method. The results indicated a positive correlation (R^2=0.8865) between the collector temperature rise above ambient ($\Delta T=T_c-T_{am}$) and the solar insolation as shown in Figure 4.9.

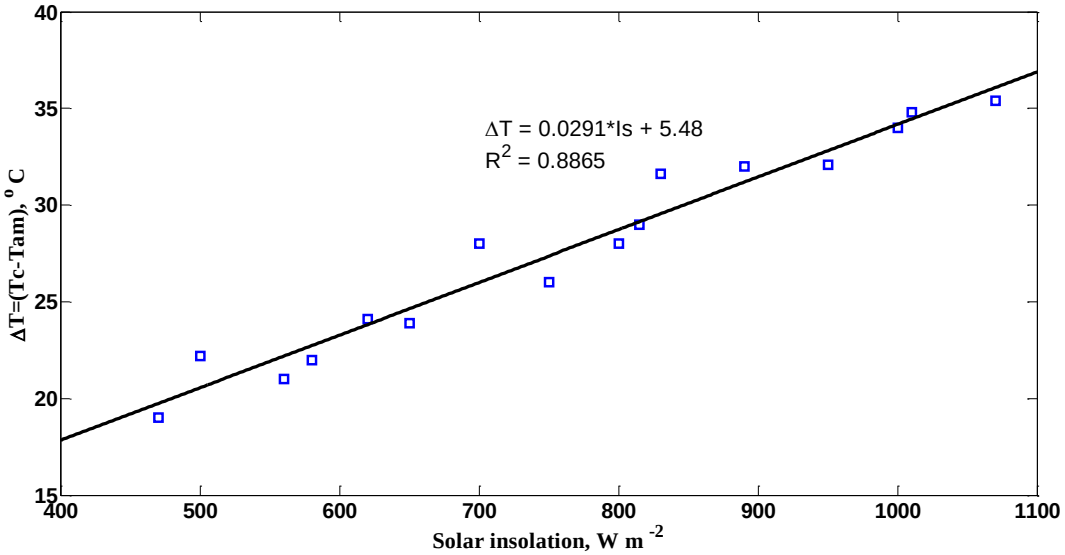

Figure 4.9: Temperature rise at the collector exit above ambient

In a study by Hossain and Bala (2002), a mean solar insolation of 800 W m^{-2} produced a mean collector temperature rise above ambient of 21.62 °C. In this study, a mean collector temperature rise above ambient of 30 °C was registered at a mean insolation of 850 W m^{-2}. This clearly shows that a significantly ($p<0.05$) higher temperature rise at the collector was recorded in this study as compared to that of Hossain and Bala (2002). From Figure 4.9, it is clear that the magnitude of air temperature rise depends on the received solar insolation, and this, most likely is the explanation of any differences in temperature rise between this study and what has been reported previously.

4.2.2 Thin layer modelling

The results from the thin layer modelling are shown in Table 4.1. The model constants and the criteria values; r^2, SSE and RMSE are also shown. The r^2, SSE and RMSE are

parameters that evaluate the goodness of fit of each model tested (Mathworks.com, 2016).

The r^2 measured how successful the fit was in explaining the variation of the data and it shows the correlation between the experimental values and the model predicted values. The r^2 varies between 0 and 1, where a value closer to 1 indicates that a greater proportion of the variance has been accounted for by the model. The SSE is a statistic that was used to indicate the total deviation of the experimental values from the fit and

a value close to 0 indicated that the model had a small random error and hence more useful for prediction.

The RMSE which is also referred to as the fit standard error of the regression was used to estimate the standard deviation of the random component of the data. Like the SSE, a value close to 0 indicated that the model fit was more useful for prediction.

From Table 4.1, all the model r^2 values were greater than 0.9 indicating their acceptability (Madamba *et al.*, 1996). By exploring further the SSE and RMSE, only one model was chosen according to the key below Table 4.1.

Table 4.1: Thin layer model results

Model No. (Refer to Table 3.2)	**Order of best fit**	**Model Coefficients**	**r^2**	**SSE $\times 10^{-3}$**	**RMSE $\times 10^{-2}$**
12	***1.***	***a = 0.9842*** ***b = 0.01614*** ***k = 0.3196*** ***n = 1.072***	***0.9959***	***4.634***	***1.758***
8	2.	a = 0.9565 g = -0.1252 k = 0.3496	0.9953	5.308	1.821
7	3.	a = 0.9565 b = -0.3585, k = 0.3496	0.9953	5.308	1.821
6	4.	a = 0.9548 b =0.04172, k0 = 0.3467 k1 = 0.1288	0.9953	5.288	1.878
5	5.	a = 0.8552 b = 0.1524 k = 0.4184	0.9926	8.274	2.274
9	6.	a = 31.82 b = 0.4129 c = -31.26 g = 0.1052 h = 0.9254 k = 0.915	0.9879	13.619	3.237
3	7.	k= 0.2764 n = 0.7553	0.9715	32.067	4.343
2	8.	a = 0.2896 k = 0.6932	0.9715	32.067	4.343
10	9.	k = 0.3787 n = 0.7553	0.9673	36.771	4.651
11	10.	a = -0.2268 b = 0.01464	0.9538	51.949	5.528
4	11.	a = 0.9327 k = 0.2503	0.9489	57.447	5.813
1	12.	k = 0.2731	0.9404	67.005	6.101

Key:1. Highest r^2, and lowest SSE and RMSE –Most accurate model

12. Lowest r^2, and highest SSE and RMSE – Least accurate model

Following the key above, Midilli-Kucuk model qualified as the best fit or most accurate model with parameters; r^2 of 0.9959, SSE of 0.004634 and RMSE of 0.01758. To show the goodness of fit by the Midilli-Kucuk model, a plot of experimental MR and Midilli-Kucuk model predicted MR against drying time was made and is presented in Figure 4.10.

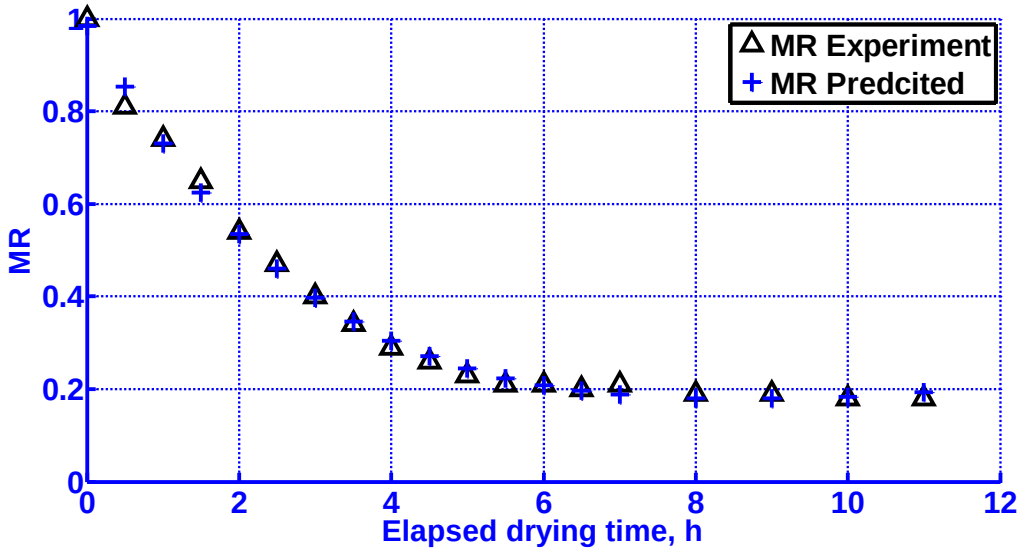

Figure 4.10: Experimental and model predicted MR

From this plot, it can be observed that the predicted and experimental MR compare well, implying that the Midilli-Kucuk model can predict with a high degree of accuracy the MR of mango as drying progresses under similar conditions shown earlier in Figures 4.7 and 4.8. The good comparison of the model and experimental MR validates the usefulness of Midilli-Kucuk model for this study. In a past study by Goyal *et al.* (2006) while drying mango in a solar tunnel, they found the Page model to be the most accurate model to predict the MR with an r^2 value of 0.9991. In this study, the Page model had an r^2 value of 0.9715. Though this value can be said to be acceptable, it was not better compared to that obtained using the the Midilli-Kucuk model (r^2 = 0.9959).

To explain the disparity in the models obtained between this study and the past study of Goyal *et al.* (2006), the following study paremeters have been pointed out:

- the tunnel dryer used in their past study was a forced convection type where the drying temperatures were controlled to only values of 55, 60 and 65 ^oC and

- the Midilli-Kucuk model was not among the models tested in their study.

In another study by Corzo *et al.* (2011) while drying green mango and half-ripe mango, the Midilli-Kucuk model was established as the most accurate model among the 10 models tested at varying temperatures ranging between 40 ^{o}C and 60 ^{o}C.

Therefore, it is worthwhile pointing out that model constants and hence the most approriate model depends on the conditons in which the study is done. The usefulness of the thin layer model established in this study may include estimating the energy cost to dry dry mango to a desired final moisture content through accurately predicting the drying time to reduce the moisture content to a desired level among others.

4.3 Evaluation of the dryer perfromance

The collector, drying and pick-up efficiencies, and the buoyancy pressure head were determined as described in the following sections. The equations described in chapter three were used to compute each of these parameters.

4.3.1 Calculation of the collector efficiency

The collector efficiency was calculated using Equation (3.8) as described in chapter three.

$$\eta_c = \frac{\dot{m}C_p\Delta T}{A_c I_s} = \frac{\dot{m}C_p(T_c - T_{am})}{A_c I_s}$$

Useful data from experiments and parameters of the dryer for the calculation is given below:

- Collector area, $\mathrm{A_c} = 0.75\ \mathrm{m^2}$
- $Mean\ solar\ insolation, I_s = 850\ W/m^2$
- $Mean\ collector\ air\ temperature\ in\ kelvin = (273.14 + 66.2) = 339.34\ K$
- $Mean\ ambient\ air\ temperature\ in\ kelvin = (273.14 + 35.68) = 308.82\ K$
- $C_p\ of\ air\ at\ mean\ collector\ air\ temperature\ (66.2\ ℃) = 1009\ J/kg\ K$
- $Air\ density\ at\ 66\ ℃, = 1.067\ kg/m^3$
- $Velocity\ of\ air\ at\ the\ collector, V_c = 0.04\ m/s$
- $Cross - sectional\ area\ of\ the\ collector, Ax$

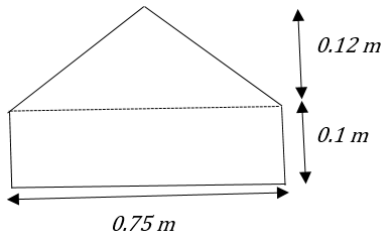

$$Ax = (0.75 \times 0.1) + \left(\left(\frac{0.75}{2}\right) \times 0.12\right) = 0.12\ m^2$$

- $\dot{m} = 0.04 \times\ 0.12 \times 1.067 = 0.0051216\ kg/s\ m^2$

Assumption

- *Air flow fills the whole cross-sectional area*

Substitution

$$\eta_c = \frac{0.0051216 \times 1009 \times (339.34 - 308.82)}{0.75 \times 850} = 0.247$$

$$\eta_c = 24.7\ \%$$

4.3.2 Calculation of the drying efficiency

The collector efficiency was calculated using Equation (3.9) described in chapter 3**.**

$$\eta_{drying} = \frac{WL}{I_{ST}A_c}$$

Useful data from experiments and parameters of the dryer for the calculation are given below:

- $Initial\ moisture\ content\ of\ mango = 80\ \%\ w.b$
- $Product\ load = 1.8\ kg$

$Therefore$;

- $Moisture\ present\ in\ mango\ initially = 0.8 \times 1.8 = 1.44\ kg$
- $Dry\ matter\ in\ mango = 0.2 \times 1.8 = 0.36\ kg$
- $Final\ moisture\ content\ of\ dried\ mango\ = 13\ \%\ w.b$
- $Moisture\ left\ in\ the\ mango\ after\ drying = \frac{0.36\times0.13}{0.87} = 0.054kg$
- $Collector\ area, A_c = 0.75\ m^2$
- $Moisture\ evaporated, W = 1.44 - 0.05 = 1.366\ kg$
- $Total\ insolation\ in\ 11\ hours, I_{sT}\ = 37981.13\ KJ\ m^{-2}$
- $Latent\ heat\ of\ water =\ 2320\ KJkg^{-1}$

Substitution

$$\eta_{drying} = \frac{1.366\times2320}{37981.13\times0.75} = 0.113$$

$$\eta_{drying} = 11.3\ \%$$

4.3.3 Calculation of the pick-up efficiency

The pick-up efficiency was calculated using Equation (3.10) as described in chapter 3.

$$\eta_{Pick\ up} = \frac{h_d - h_c}{h_{as} - h_c}$$

Useful data from experiments and parameters of the dryer used for the calculation are given below:

- ***Mean collector air conditons***
  - $Mean\ collector\ air\ temperature = 66.2$ ℃
  - $Mean\ collector\ air\ relative\ himidity =$ 6.4 %
- ***Mean drying unit air conditons***
  - $Mean\ drying\ unit\ air\ temperature =$ 54.7 ℃
  - $Mean\ drying\ unit\ air\ relative\ himidity =$ 8.4 %

From the mean air conditions at the collector and drying unit and using a psychrometric chart, the absolute humidity corresponding to mean air and relative humidity were obtained:

- $h_d = 0.017\ kg/kg$
- $h_c = 0.01\ kg/kg$
- $h_{as} = 0.03\ kg/kg$

Substitution

$$\eta_{Pick\ up} = \frac{0.017 - 0.01}{0.03 - 0.01} = 0.35$$

$$\eta_{Pick\ up} = 35\%$$

As calcualted above, the collector, drying and pick-up efficiencies were found to be 24.7 %, 11.3 % and 35 % respectively. Though the obtained efficiencies appeared to be numerically low, they were sufficient for drying the mango in one and half typical drying days to moisture contents of between 13 and 14 % (w.b.) from 80 % (w.b.).

Research carried out by Brenndorfer *et al.* (1987) estimated the typical drying efficiency of natural convection dryers to be in the range of 10 and 15 %. Therefore, the drying efficiency of 11.3 % found in this study was marginally above the typical lower limit. One possible explanation for the marginally low drying efficiency is that the recommended loading rate for mango of 2.6 kg m^{-2} used in this study was probably low considering the attained conditions by the dryer. For example, the average relative humidity of the air leaving the drying unit was relatively low at only 8.4 % meaning

the air still had a high moisture carrying capacity. Assuming that the loading rate was increased above 2.6 kg m^{-2} and the same drying time of 11 hours obtained under the new loading rate and following the calculation of the drying effieciency above, the new drying efficiency would be expected to be higher than the obtained value of 11.3 %.

In a study by Schiavone (2011) while evaluating a natural convection solar dryer, efficiencies of 29.05 %, 10.8 % and 33.9 % for the collector, drying and pick-up efficiencies respectively were obtained. These efficiencies were not significanlty different from the values obtained in this study and therefore, it can be infered that natural convection systems are generallycharacterised by low efficiences even when satisfactory drying times are achieved.

4.3.4 Buoyancy pressure head

From the mathematical relationship of buoyancy pressure head and air temperature defined in Chapter 3 (Equation 3.12), the buoyancy pressure head developed by the chimney was calculated and its variation with the received solar insolation was plotted as shown in Figure 4.11.

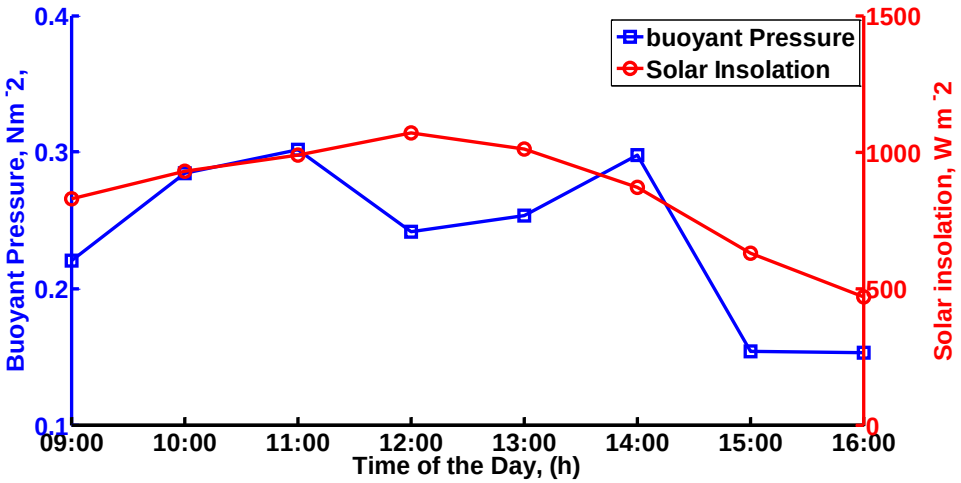

Figure 4.11: Buoyancy pressure head and solar irradiance as a function of time

Due to the dependance of the air temperatures in the dryer on the recieved solar insolation, the buoyancy pressure followed a simialr pattern to that of the solar insolation. With an average temperature rise above ambient of about 7.7 ^{o}C at the

chimney seen earlier in Figure 4.7, the boyancy pressure head ranged between 0.3016 and 0.1530 N m^{-2} which was sufficient to drive the air in the dryer throughout the drying periods.

The wind pressure which adds to the developed buoyancy pressure to drive air flow in natural convective dryers was considered negligable in this study for two reasons and these were;

i. the air velocities which define the wind pressure were low with V_{am} and V_c averaging 0.36 m s^{-1} and 0.04 m s^{-1} respectively and
ii. on the extreme cases, air movements could momentarily reduce to values close to zero and this implies that the air flow was entirely dependent on the buoyancy pressure head.

Experimental results of Schiavone (2011) in a natural convection solar dryer indicated that the registered air velocity of 0.4 m s^{-1} inside the dryer was significanlty ($p<0.05$) higher than the registered value in this study. Despite the relatively high velocity inside the dryer in his study, its effect in contributing to air flow was negligable compared to the effect produced by the buoyancy pressure difference of 1.91 Pa. Therefore, natural convection dryers suffer low air velocities due to low air pressure and therefore this requires that the chimney heats the air to significanlty high values above ambient to cause enough buoyancy pressure for air flow.

4.4 Closing remarks

The results and discussions of the study were covered in this chapter. Relevant literarure to back up the findings of the study have been provided as much possible. In general, the specific objectives were met as the dryer was constructed, tested and evaluated based on the parameters that were defined in the study.

CHAPTER FIVE

5 CONCLUSIONS AND RECOMMENDATIONS

This chapter presents the conclusions and recommendations drawn from the study. The conclusions have been presented to reflect the achievement of each specific objective and for clarity purposes.

5.1 Conclusions

- **To construct a natural convection solar tunnel dryer for experimentation**
  - A natural convection solar tunnel dryer was constructed and tested with mango as the product.
  - The constructed solar tunnel dryer was simple and fairly affordable having a basic cost of only K 433 as seen from Appendix I
- **To determine an appropriate mathematical thin layer model to predict the drying characteristic of mango and validate it against experimental results**
  - A total 9 experiments were done in the solar tunnel dryer where the first 5 experiments were dry runs while the last four were mango drying experiments.
  - From the dry run experiments, it was found necessary to modify the dryer air inlet point by incorporation of an air guide because an anomalous phenomenon that has been described as bidirectional air flow was experienced without an air guide.
  - After incorporation of the air guide, a unidirectional air flow was achieved. With the modification in place, the mango moisture content of 80 % (w.b.) was reduced to between 13 and 14 % (w.b.) in only 11 hours. This is because the dryer conditioned the ambient air inside the dryer achieving a collector temperature of up to 70 °C and low relative humidity as low as 6 %.
  - Under the registered natural conditions, a thin layer mathematical model was established to help predict the drying of mango and validated against experimental results. Midilli-Kucuk model was established as the most accurate model as it compared well with experimental results. The goodness of fit parameters were; r^2, SSE and RMSE of 0.9959, 0.004634 and 0.01758 respectively.
- **To evaluate the collector efficiency, drying efficiency, pick-up efficiencies and attainable buoyancy pressure by the chimney**

- Besides the drying time as one of the performance evaluation parameters for the dryer, the collector, drying and pick-up efficiencies were calculated and found to be 4.7 %, 11.3 % and 35 % respectively which were typical of natural convection dryers according to the reviewed literature. Although the chimney air temperature above ambient was below 10 °C, its performance was sufficient in driving the flow of air.
- From the above conclusions, the natural convection solar tunnel dryer is well suited for both small scale and commercial drying of mango.

5.2 Recommendations

The following recommendations were drawn from this study.

1) A loading density greater than the recommended 2.6 kg/m^2 can be used in this dryer because of the observed relatively low humidity of the air leaving the drying unit and the low drying efficiency.
2) For a much higher temperature rise at the chimney unit greater than the observed mean value of 7.7 °C, the chimney unit may be modified from the bare flat-plate to a covered flat-plate type in order to reduce the heat losses and subsequently increase the thermal efficiency.
3) To confidently use this dryer for other fruits such as bananas, pineapple etc., experimentation of the dryer using these fruits is necessary in order to find the drying time to equilibrium.
4) Another potential study area in this constructed dryer is comparison of the dryer performance for different slice thicknesses of the same product.

5.3 Closing remarks

This chapter provides the conclusions and the recommendations from the study. The conclusions have been linked to the set specific objectives in order to enhance clarity while the recommendations section has attempted to point out some gaps that need to be investigated by subsequent researches.

REFERENCES

Ahmad, A., Saini, J. & Varma, H. 1996. Thermohydraulic performance of packed-bed solar air heaters. *Energy conversion and Management,* 37**,** 205-214.

Ajila, C., Bhat, S. & Rao, U. P. 2007. Valuable components of raw and ripe peels from two Indian mango varieties. *Food Chemistry,* 102**,** 1006-1011.

Akoy, E., Ismail, M. A., Ahmed, E.-F. A. & Luecke, W. 2006. Design and construction of a solar dryer for mango slices. *Proceedings of International Research on Food Security, Natural Resource Management and Rural Development-Tropentag. University of Bonn, Bonn, Germany*.

Akpinar, E. K. 2006. Determination of suitable thin layer drying curve model for some vegetables and fruits. *Journal of food engineering,* 73**,** 75-84.

AOAC 2005. *Official methods of analysis,* Washington DC: Association of Official Analytical Chemists International

Bala, B., Mondol, M., Biswas, B., Chowdury, B. D. & Janjai, S. 2003. Solar drying of pineapple using solar tunnel drier. *Renewable Energy,* 28**,** 183-190.

Belessiotis, V. & Delyannis, E. 2011. Solar drying. *Solar Energy,* 85**,** 1665-1691.

Brenndorfer, B., Kennedy, L. & Mrema, G. 1987. *Solar dryers: their role in post-harvest processing*, Commonwealth Secretariat.

Corzo, O., Bracho, N. & Alvarez, C. 2011. Determination of suitable thin layer model for air drying of mango slices (Mangifera indica L.) at different air temperatures and velocities. *Journal of Food Process Engineering,* 34**,** 332-350.

Dissa, A., Bathiebo, J., Kam, S., Savadogo, P., Desmorieux, H. & Koulidiati, J. 2009. Modelling and experimental validation of thin layer indirect solar drying of mango slices. *Renewable Energy,* 34**,** 1000-1008.

Doymaz, I. 2004. Effect of pre-treatments using potassium metabisulphide and alkaline ethyl oleate on the drying kinetics of apricots. *Biosystems Engineering,* 89**,** 281-287.

Duffie, J. A. & Beckman, W. A. 1980. *Solar engineering of thermal processes,* Wiley New York etc.

Ekechukwu, O. & Norton, B. 1997. Design and measured performance of a solar chimney for natural-circulation solar-energy dryers. *Renewable energy,* 10**,** 81-90.

Ekechukwu, O. & Norton, B. 1999a. Review of solar-energy drying systems II: an overview of solar drying technology. *Energy conversion and management,* 40**,** 615-655.

Ekechukwu, O. & Norton, B. 1999b. Review of solar-energy drying systems III: low temperature air-heating solar collectors for crop drying applications. *Energy Conversion and Management,* 40**,** 657-667.

El-Sebaii, A., Aboul-Enein, S., Ramadan, M. & El-Gohary, H. 2002. Experimental investigation of an indirect type natural convection solar dryer. *Energy Conversion and Management,* 43**,** 2251-2266.

Esper, A., Lutz, K. & Mühlbauer, W. 1989. Development and testing of plastic film solar air heaters. *Solar and wind technology,* 6**,** 189-195.

FAO, F. 2013. Statistical Yearbook 2013: World Food and Agriculture. *FAO Food Agric. Organziation UN Rome Italy*.

Forson, F., Nazha, M., Akuffo, F. & Rajakaruna, H. 2007. Design of mixed-mode natural convection solar crop dryers: Application of principles and rules of thumb. *Renewable Energy,* 32**,** 2306-2319.

Fudholi, A., Sopian, K., Ruslan, M. H., Alghoul, M. & Sulaiman, M. Y. 2010. Review of solar dryers for agricultural and marine products. *Renewable and Sustainable Energy Reviews,* 14**,** 1-30.

Gayanilo, V. G. 1980. A solar-heated grain dryer for the tropics.

Goyal, R., Kingsly, A., Manikantan, M. & Ilyas, S. 2006. Thin-layer drying kinetics of raw mango slices. *Biosystems Engineering,* 95**,** 43-49.

Grainger, W., Othieno, H. & Twidel, J. 1981. Small scale solar crop dryers for tropical village use-theory and practical experiences. ISES, Solar World Forum, Brighton, UK. *Pergamon Press, Oxford,* 1981**,** 989-96.

Hichaambwa, M. 2010. Developments in the Horticultural supply chains in Zambia. *Food Security Research Project (FSRP), Lusaka*.

Hodges, R. J., Buzby, J. C. & Bennett, B. 2011. Postharvest losses and waste in developed and less developed countries: opportunities to improve resource use. *The Journal of Agricultural Science,* 149**,** 37-45.

Hossain, M. & Bala, B. 2002. Thin-layer drying characteristics for green chilli. *Drying Technology,* 20**,** 489-505.

Hossain, M. & Bala, B. 2007. Drying of hot chilli using solar tunnel drier. *Solar Energy,* 81**,** 85-92.

Hossain, M., Woods, J. & Bala, B. 2005. Optimisation of solar tunnel drier for drying of chilli without color loss. *Renewable energy,* 30**,** 729–742.

Kader, A. A. Increasing food availability by reducing postharvest losses of fresh produce. V International Postharvest Symposium 682, 2004. 2169-2176.

Kiaya, V. 2014. Post-harvest losses and strategies to reduce them. *New York: Action Contre la Faim (ACF International)*.

Kitinoja, L., AlHassan, H., Saran, S. & Roy, S. 2010. Identification of appropriate postharvest technologies for improving market access and incomes for small horticultural farmers in Sub-Saharan Africa and South Asia. Part.

Kuteya, A. 2012. Agricultural Policies and Food Security Challenges in Zambia. April 2012 ed.

Lahsasni, S., Kouhila, M., Mahrouz, M., Idlimam, A. & Jamali, A. 2004. Thin layer convective solar drying and mathematical modeling of prickly pear peel (Opuntia ficus indica). *Energy,* 29**,** 211-224.

Leon, M. A., Kumar, S. & Bhattacharya, S. 2002. A comprehensive procedure for performance evaluation of solar food dryers. *Renewable and Sustainable Energy Reviews,* 6**,** 367-393.

Mackay, M. E. 2015. *Solar Energy An Introduction,* USA, Oxford University Press 198 Madison Avenue, New York, NY 10016, United States of America.

Madamba, P. S., Driscoll, R. H. & Buckle, K. A. 1996. The thin-layer drying characteristics of garlic slices. *Journal of food engineering,* 29**,** 75-97.

Mastekbayeva, G. A., Bhatta, C. P., Leon, M. A. & Kumar, S. 1999. Experimental studies on a hybrid dryer. *ISES Sol World Cong, Israel***,** 4-9.

Mastekbayeva, G. A., Leon, M. A. & Kumar, S. Performance evaluation of a solar tunnel dryer for chilli drying. Asean Seminar and Workshop on Solar Drying Technology, 1998. 3-5.

Mathworks.com. 2016. *Evaluating Goodness of Fit* [Online]. [Online] Available at: https://www.mathworks.com/help/curvefit/evaluating-goodness-of-fit.html. [Accessed Accessed 05th Oct 2016 2016].

Midilli, A., Kucuk, H. & Yapar, Z. 2002. A new model for single-layer drying. *Drying technology,* 20**,** 1503-1513.

Mohanraj, M. & Chandrasekar, P. 2008. Drying of copra in a forced convection solar drier. *Biosystems engineering,* 99**,** 604-607.

Mujumdar, A. S. & Devahastin, S. 2000. Fundamental principles of drying. *Exergex, Brossard, Canada*.

Mundia, F. 2004. National Agricultural Policy (2004 - 2015). *In:* CO-OPERATIVES, M. O. A. A. (ed.).

Pala, M., Mahmutoğlu, T. & Saygi, B. 1996. Effects of pretreatments on the quality of open-air and solar dried apricots. *Food/Nahrung,* 40**,** 137-141.

Pangavhane, D. R., Sawhney, R. & Sarsavadia, P. 2002. Design, development and performance testing of a new natural convection solar dryer. *Energy,* 27**,** 579-590.

Parfitt, J., Barthel, M. & Macnaughton, S. 2010. Food waste within food supply chains: quantification and potential for change to 2050. *Philosophical Transactions of the Royal Society of London B: Biological Sciences,* 365**,** 3065-3081.

Purohit, P., Kumar, A. & Kandpal, T. C. 2006. Solar drying vs. open sun drying: A framework for financial evaluation. *Solar Energy,* 80**,** 1568-1579.

Sacilik, K., Keskin, R. & Elicin, A. K. 2006. Mathematical modelling of solar tunnel drying of thin layer organic tomato. *Journal of Food Engineering,* 73**,** 231-238.

Schiavone, F. 2011. *Development and Evaluation of a Natural Convection Solar Dryer For Mango in Rural Haitian Communities.* Msc. Thesis, Univeristy of Florida.

Schirmer, P., Janjai, S., Esper, A., Smitabhindu, R. & Mühlbauer, W. 1996. Experimental investigation of the performance of the solar tunnel dryer for drying bananas. *Renewable Energy,* 7**,** 119-129.

Sharma, A., Chen, C. & Lan, N. V. 2009. Solar-energy drying systems: A review. *Renewable and sustainable energy reviews,* 13**,** 1185-1210.

Shaw, D. J. 2007. World Food Summit, 1996. *World Food Security.* Springer.

Simate, I. N. 2003. Optimization of mixed-mode and indirect-mode natural convection solar dryers. *Renewable Energy,* 28**,** 435-453.

Simon, P. 2011. *Crop Production Science in Horticulture Series,* CAB International 2011.

Soponronnarit, S., Subannapong, W. & Tiansuwan, J. 1990. Studies of Bare and Glass-Cover Flat-Plate Solar Air Heaters. *RERIC International Energy Journal,* 12**,** 1-19.

Sparrow, E. & Bahrami, P. 1980. Experiments on natural convection from vertical parallel plates with either open or closed edges. *Journal of Heat Transfer,* 102**,** 221-227.

Statisticssolutions.com. 2016. *How to Conduct Linear Regression* [Online]. Available at: http://www.statisticssolutions.com/how-to-conduct-linear-regression/. [Accessed Accessed 05th Oct 2016 2016].

Tiris, C., Tiris, M. & Dincer, I. 1995. Investigation of the thermal efficiencies of a solar dryer. *Energy conversion and management,* 36**,** 205-212.

Touré, S. & Kibangu-Nkembo, S. 2004. Comparative study of natural solar drying of cassava, banana and mango. *Renewable Energy,* 29**,** 975-990.

Weiss, W. & Buchinger, J. 2012. Solar Drying. *AEE INTEC Publication, A-8200 Gleisdorf, Feldgasse,* 19.

Weiss, W. & Rommel, M. 2008. Process heat collectors. *State of the Art within Task,* 33.

Appendix I: Materials used for the dryer

No.	Material	Unit	Cost per Unit (K/Unit)	Number of units/Quantity	Total Cost (K)
1	Galvanised Iron	2 m×0.915 m	79	3.26 m^2	139.0
2	Green house plastic	1 m^2	13.74	2.60 m^2	36.0
3	Wire mesh trays	15 m×1.2 m	700	0.75 m^2	30.0
4	Mosquito wire gauge	1.2 m×1 m	10	0.15 m^2	1.25
5	Matt black paint	125 ml	65	1.00	65.0
6	Square tube	20 mm×20 mm×6 m	45	12.0 m	90.0
8	Rivets	100 pack(3.2 mm×8 mm)	25	1 pack	25.0
9	Flat bar	20 mm×3 mm× 6m	35	8 m	46.7
	Total				**433**

Appendix II: Collector and drying units

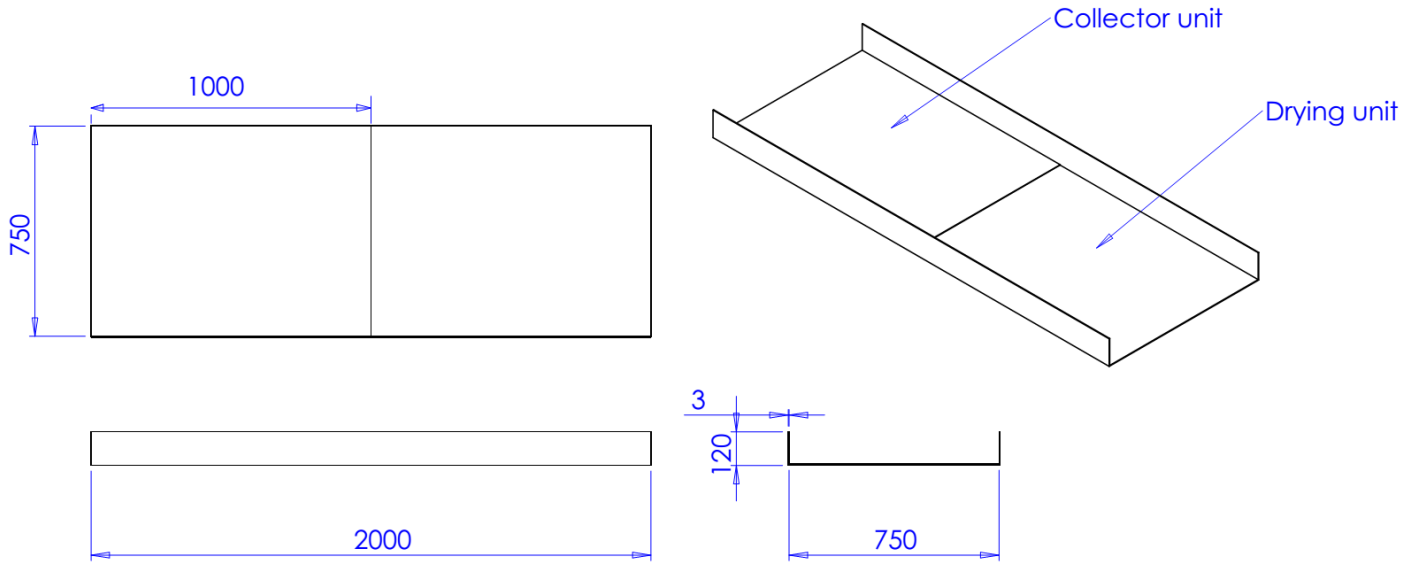

DRAWN BY	SAM CHEROTICH		SCALE	1:20
CHECKED BY	Dr. ISAAC N. SIMATE		UNITS	mm
SIGNATURE		TITLE	COLLECTOR AND DRYER UNITS	
DATE		MATERIAL	0.3 mm GALVANIZED IRON	

Appendix III: Drying tray

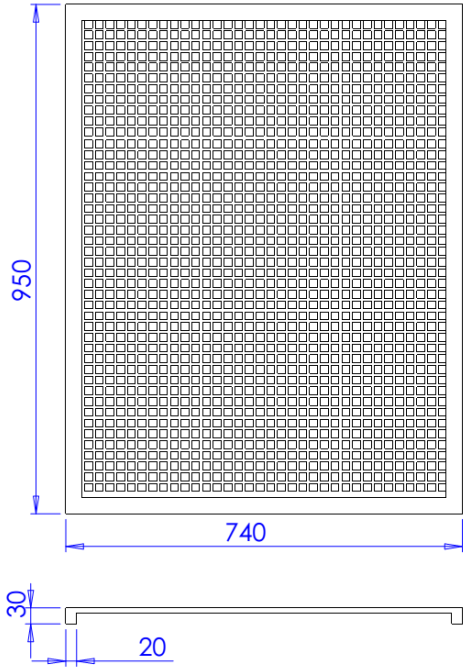

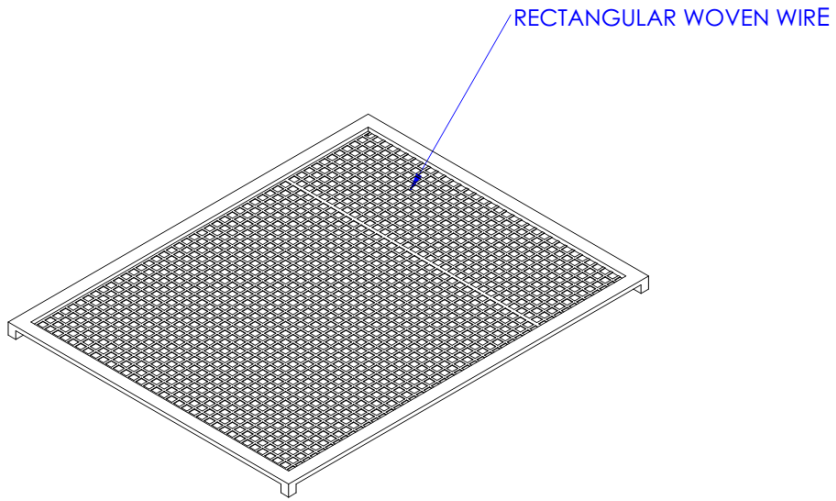

DRAWN BY	SAM CHEROTICH		SCALE	1:20
CHECKED BY	Dr. ISAAC N. SIMATE		UNITS	mm
SIGNATURE		TITLE	DRYING TRAY	
DATE		MATERIAL	STEEL	

Appendix IV: Chimney unit

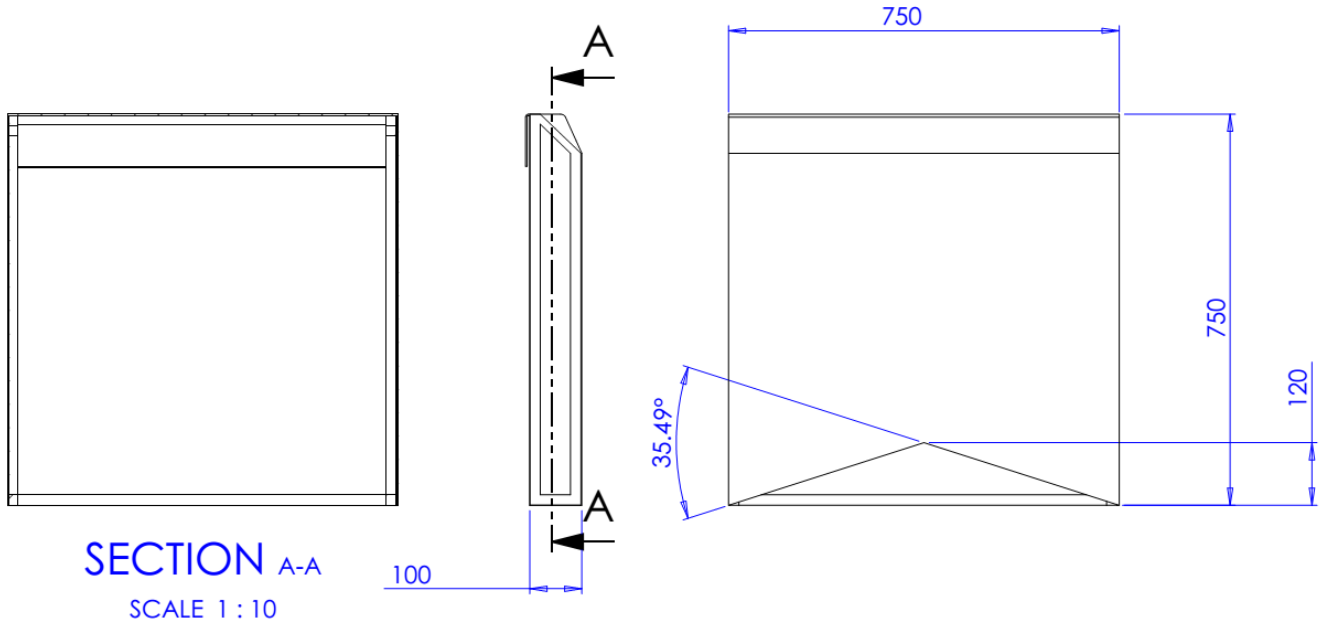

DRAWN BY	SAM CHEROTICH		SCALE	1:10
CHECKED BY	Dr. ISAAC N. SIMATE		UNITS	mm
SIGNATURE		TITLE	Chimney Unit	
DATE		MATERIALS	0.3 mm GALVANIZED IRON AND SQUARE TUBE	

Appendix V: Dryer stand/Legs

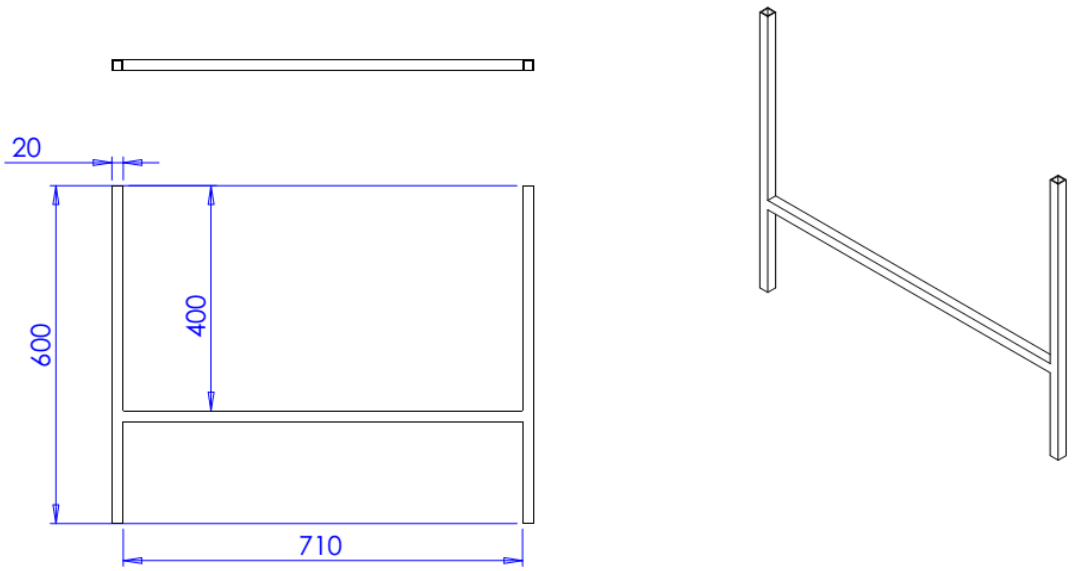

DRAWN BY	SAM CHEROTICH		SCALE	1:5
CHECKED BY	Dr. ISAAC N. SIMATE		UNITS	mm
SIGNATURE		TITLE	COLLECTOR AND DRYER UNITS	
DATE		MATERIAL	20 × 20 mm steel tube	

Appendix VI: Elbow join

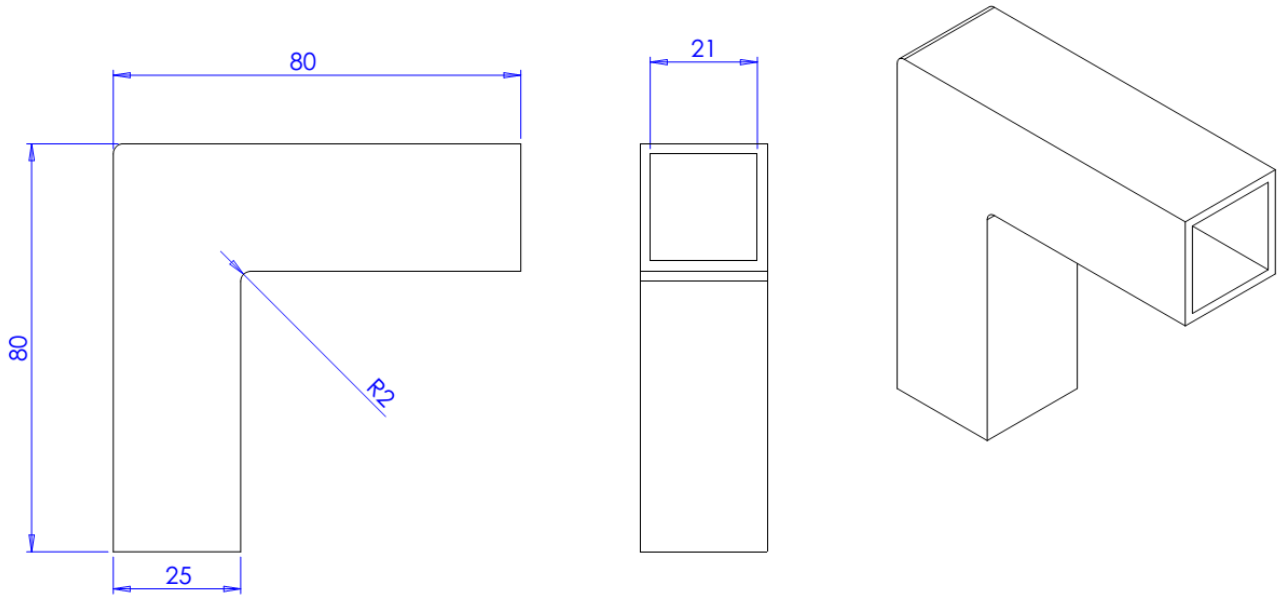

DRAWN BY	SAM CHEROTICH		SCALE	1:1
CHECKED BY	Dr. ISAAC N. SIMATE		UNITS	mm
SIGNATURE		TITLE	ELBOW JOIN	
DATE		MATERIAL	STEEL	

Appendix VII: Air guide

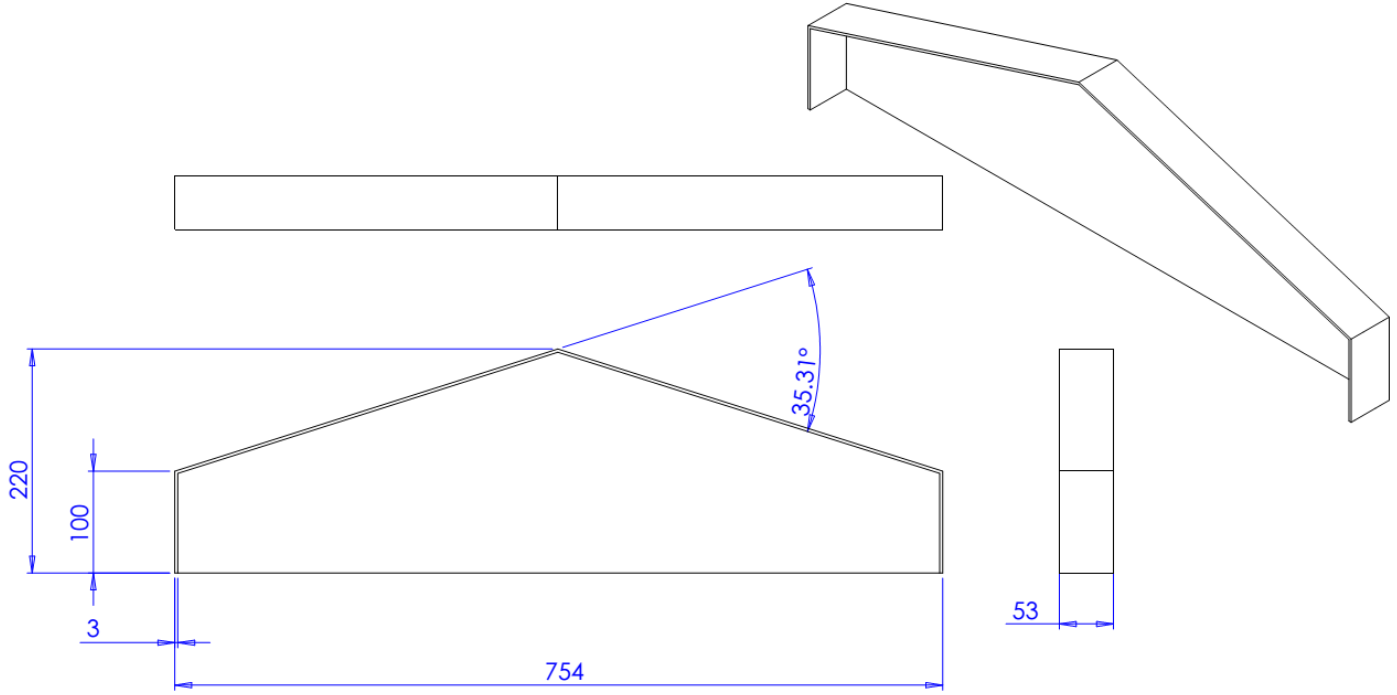

DRAWN BY	SAM CHEROTICH		SCALE	1:5
CHECKED BY	Dr. ISAAC N. SIMATE		UNITS	mm
SIGNATURE		TITLE	Air guide	
DATE		MATERIAL	0.3 mm GALVANIZED IRON	

Appendix VIII: 3-D Assembly of the solar tunnel dryer

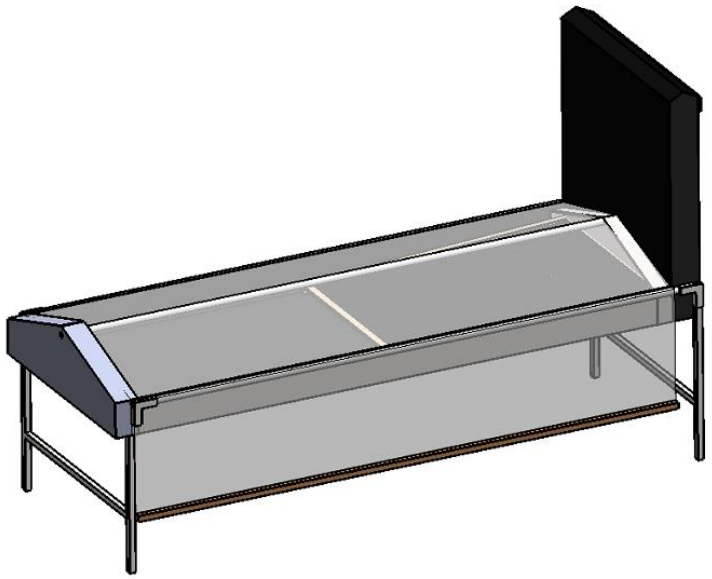

DRAWN BY	SAM CHEROTICH		SCALE	1:10
CHECKED BY	Dr. ISAAC N. SIMATE		UNITS	mm
SIGNATURE		TITLE	3-D ASSEMBLY	
DATE		MATERIAL		

Appendix IX: Sample calculation of the reduction in PHLs

The dryer used in this study was a small solar tunnel dryer with a loading capacity of 1.8 kg of mango. However, this was for experimental purposes only. Bigger size dryers are possible with sizes of up to 10 square meters dryer unit size. To estimate PHLs, some assumptions were made and the estimate shown in Appendix X.

Assumptions

1. The mango dried is the mango that would otherwise go to waste.
2. The dyer was operated for 90 days (3 months), a period when mango is available after harvest

The calculations

The dryer achieved a drying time of only 11 hours requiring two typical drying days. Therefore, number drying runs in the 90 days

$$Drying\ runs\ = \frac{Number\ of\ drying\ days\ available}{Required\ drying\ time\ (days)}$$

$$= \frac{90}{2}$$

$$= 45$$

$$Redcution\ in\ PHLs\ = Dryer\ loading\ capacity\ (kg/m^2)\ / \times drying\ runs$$

$$= 1.8\ \times 45$$

$$= 1.8\ \times 45$$

$$= 81\ kg\ per\ \ square\ meter\ per\ dryer$$

Appendix X: Estimated reduction in PHLs for different dryer sizes

Size of drying unit (m^2)	Loading capacity kg/m^2	Available drying time (Days)	Possible drying runs	Reduction in PHLs kg
1	1.8	90	45	81
2	3.6	90	45	162
4	7.2	90	45	324
8	14.4	90	45	648
10	18	90	45	810

Appendix XI: Definitions related to solar energy reception on the earth

Term	Definition
Beam Radiation	The solar radiation received from the sun without having been scattered by the atmosphere. Beam radiation is often referred to as direct solar radiation. It is measured in Wm^{-2}
Diffuse radiation	The solar radiation received from the sun after its direction has been changed through scattering by the atmosphere. Diffuse radiation is sometimes referred to as sky radiation or solar sky radiation. It is measured in Wm^{-2}.
Total Solar Radiation	This is the sum of beam and the diffuse solar radiation on a surface. The most common measurements of solar radiation are total radiation on a horizontal surface, often referred to as global radiation on the surface. The units are Wm^{-2}
Irradiance	The rate at which radiant energy is incident on a surface per unit area of surface. It is measured in $W\ m^{-2}$
Insolation	This is a term applying specifically to solar energy irradiation. The units are Wm^{-2}
Transmissivity	This is the fraction of the radiation incident on a material permitted to go through and it ranges between 0 and 1 (dimensionless)
Absorptivity	This is the fraction of incident solar radiation absorbed by a surface and ranges between 0 and 1(dimensionless)

Source:(Duffie and Beckman, 1980)